Deciphering the role of PE_PGRS45 (Rv2615c) protein of Mycobacterium tuberculosis in host macrophage apoptosis: Possible effector for persistence

Monika Sharma[1], * Medha[1], * Priyanka[1], and Sadhna Sharma[1]

[1]University of Delhi Miranda House

January 26, 2023

Abstract

Mycobacterium tuberculosis has co-evolved with its host to evade and modulate host cellular processes. Few PE/PPE proteins of *Mycobacterium* have been reported to modulate cell death pathways and determine the infection outcome. This study investigates role of one such uncharacterized protein PE_PGRS45/Rv2615c in host cell death and immuno-modulation. *In-silico* analysis predicted similarity of Rv2615c with APAF1-apoptosome and involvement in Cysteine-type endo-peptidase activation during apoptosis. *In-vitro* experiments with THP-1 macrophages confirmed the Caspase-dependent apoptosis inducing potential of Rv2615c. Several PE_PGRS proteins have been reported to be TLR-agonist. Docking showed preferential binding of Rv2615c with TLR4 than TLR2. Up-regulation of TLR4-HLA-DR-MyD88-NF-B-TNF-α in Rv2615c-stimulated THP-1 macrophages was observed. To investigate the mechanism underpinning the apoptotic function, a thorough sequence scan of Rv2615c revealed the presence of eukaryotic CARD-like domain in it. *In-silico* studies showed binding affinity of Rv2615c's CARD-like domain with APAF1-CARD and Caspase9-CARD, attributing Rv2615c's role in apoptosis. Since, Rv2615c is reported to be upregulated in dormancy which suggest that it may be one of the unexplored effectors employed by Mtb for its persistence via silent cell-to-cell spread of infection by inducing macrophage apoptosis. Additionally, Rv2615c's interaction with TLR4 implicates its engagement in host-pathogen interaction.

Deciphering the role of PE_PGRS45 (Rv2615c) protein of *Mycobacterium tuberculosis* in host macrophage apoptosis: Possible effector for persistence

Medha , Priyanka, Sadhna Sharma, Monika Sharma*

DSKC Bio Discovery Lab and

Department of Zoology, Miranda House, University of Delhi, New Delhi, India- 110007

***Corresponding author: Dr. Monika Sharma**

Address: Department of Zoology, Miranda House, University of Delhi, Delhi, India – 110007

Email- monika.sharma@mirandahouse.ac.in (*Correspondence and reprints")

Other Contacts – medha1.singh@mirandahouse.ac.in , priyanka.taank@mirandahouse.ac.in, sadhna.sharma@mirandahouse.ac.in

Running Title:

PE_PGRS45 protein induces host macrophage apoptosis

Summary

Mycobacterium tuberculosis has co-evolved with its host to evade and modulate host cellular processes. Few PE/PPE proteins of*Mycobacterium* have been reported to modulate cell death pathways and determine the infection outcome. This study investigates role of one such uncharacterized protein PE_PGRS45/Rv2615c in host cell death and immuno-modulation. *In-silico* analysis predicted similarity of Rv2615c with APAF1-apoptosome and involvement in Cysteine-type endo-peptidase activation during apoptosis. *In-vitro* experiments with THP-1 macrophages confirmed the Caspase-dependent apoptosis inducing potential of Rv2615c. Several PE_PGRS proteins have been reported to be TLR-agonist. Docking showed preferential binding of Rv2615c with TLR4 than TLR2. Up-regulation of TLR4-HLA-DR-MyD88-NF-B-TNF-α in Rv2615c-stimulated THP-1 macrophages was observed. To investigate the mechanism underpinning the apoptotic function, a thorough sequence scan of Rv2615c revealed the presence of eukaryotic CARD-like domain in it. *In-silico* studies showed binding affinity of Rv2615c's CARD-like domain with APAF1-CARD and Caspase9-CARD, attributing Rv2615c's role in apoptosis. Since, Rv2615c is reported to be upregulated in dormancy which suggest that it may be one of the unexplored effectors employed by Mtb for its persistence via silent cell-to-cell spread of infection by inducing macrophage apoptosis. Additionally, Rv2615c's interaction with TLR4 implicates its engagement in host-pathogen interaction.

Keywords:

Mycobacterium tuberculosis, Rv2615c, Apoptosis, Toll-like receptor 4, CARD-like domain

Abbreviation:

Mycobacterium tuberculosis (Mtb), Apoptotic Peptidase Activating Factor 1 (APAF1), Caspase Activation and Recruitment Domains (CARD), Toll-like receptor (TLR), Tumor necrosis factor-α (TNF-α)

1. Introduction

Tuberculosis (TB) caused by intracellular bacterium *Mycobacterium tuberculosis* (Mtb), remains a global health burden for decades now (WHO, 2021). Many hypothetical proteins in different pathogenic bacteria have been characterized and found to play role in pathogen persistence and disease progression suggesting the importance of unravelling their function (Desler *et al.* , 2009; Kumar *et al.* , 2014). The Proline-Glutamate (PE)/ Proline-Proline-Glutamate (PPE) proteins encoded within 7% of Mtb genome are exclusive to the pathogenic*Mycobacterium* (Cole *et al.* , 1998; Gey Van Pittius *et al.* , 2006; McGuire *et al.* , 2012). The PE_-PGRS proteins of this family have been studied for their immunogenic potential and as modulators of host immune responses (Medha, Sharma and Sharma, 2021). Many PE_PGRS proteins are still uncharacterized and therefore, investigating their role in Mtb pathogenesis and persistence poses an interesting research question.

Various cell death modalities such as necrosis, pyroptosis, autophagy and apoptosis have been reported in case of Mtb infection which are immune defence mechanisms of host (Chai, Wang and Liu, 2020). It is important to understand how these cell death modalities are exploited by the pathogen for its benefit. There are approximately 12 PE_PGRS proteins observed to be expressed a late stage of infection (chronic stage) i.e., at 90 days in infected guinea pig lungs (Kruh *et al.* , 2010). A recent study investigated the role of PE_PGRS5 and revealed the ability of this late stage expressing protein to induce apoptosis (Grover *et al.* , 2018). Reports on other PE proteins such as PE_PGRS33 and PE6 have also shown the apoptosis inducing potential of these Mtb proteins; though the time of their expression is yet to be investigated (Basu *et al.* , 2007) (Sharma *et al.* , 2021). The apoptogenic function played by these PE family proteins has been discussed to be beneficial for granuloma maintenance during later stages and infection persistence in all the reported studies. On the basis of these findings, we deduced that these PE/PPE proteins might be expressed at later stages of infection within granuloma of infected host cell. Apoptosis induction by these proteins may enable Mtb to expand its niche without an exaggerated inflammatory response to promote its persistence (Medha, Sharma and Sharma, 2021). It has been reported that Mtb escapes the phagolysosome and translocate to cytosol where it triggers host cell apoptosis. These apoptotic cells can be phagocytosed by naïve infiltrated macrophages which accumulate to develop primary granulomatous lesion. The bacilli infected macrophages then migrate to different tissues and culminates in secondary granuloma development. Findings

of studies on Mtb infected mouse and zebrafish lung granuloma suggest that apoptosis and bacilli survival could be positively correlated; though needs further research (Davis *et al.* , 2002), (Volkman *et al.* , 2004), (Saunders and Britton, 2007), (Seimon *et al.* , 2010), (Ramakrishnan, 2012). Mtb-infected lung granulomas have reported to contain apoptotic macrophages. (Fayyazi *et al.* , 2000; Pan *et al.* , 2005). While some studies showed apoptosis as a host mediated defence mechanism against the pathogens; recent studies also showed that several Mtb proteins could either induce or inhibit apoptosis. Therefore, if Mtb has both apoptogenic as well as apoptosis inhibiting proteins, it is important to understand when these proteins express themselves during the course of infection. When the apoptosis induction potential of these proteins was correlated with their time of expression, it was observed that these proteins might be expressed at late stages of infection at the site of lung granuloma and aid in pathogen dissemination via apoptosis (Grover *et al.* , 2018) (Sharma *et al.* , 2021). Additionally, one study also revealed that to prevent excessive host inflammatory responses and ensure long-term intracellular survival, Mtb regulates intracellular bacterial burden by inducing apoptosis (Chai*et al.* , 2019). The PE PGRS proteins and the ESX-V secretory system have co-evolved together and it has been reported that members of ESX-I and ESX-V secretory system induce host cell apoptosis that aids in pathogen persistence (Gey Van Pittius *et al.* , 2006), (Abdallah*et al.* , 2007), (Abdallah *et al.* , 2011), (Aguilo *et al.* , 2013). PE_PGRS33 (Rv1818c) has been reported to trigger mitochondria-mediated intrinsic apoptosis via TLR2-TNF-α signalling and facilitates survival of *Mycobacterium smegmatis* expressing this protein within host macrophages (Basu *et al.* , 2007) (Cadieux*et al.* , 2011). Another protein Rv0297 [PE_PGRS5] expressed at 90 days of infection is reported to induce endoplasmic reticulum stress mediated apoptosis via TLR4-TNF-α signalling pathway and favours Mtb dissemination (Grover *et al.* , 2018).

In TDR Target database, Rv2615c is reported to be an essential protein in Mtb growth and is up-regulated during latent/dormant TB infection (Hasan *et al.* , 2006; Murphy and Brown, 2007). Biochemical characterization of Rv2615c revealed it to be an oxidoreductase which could be targeted by drugs with anti-TB property using drug repurposing approach (Medha, Joshi, *et al.* , 2022). Given the essentiality of this protein in Mtb pathogenesis, we designed this study to investigate the molecular characterization of Rv2615c (PE_PGRS45) protein in host cell death and in modulation of host immune response. Preliminary*in-silico* profiling predicted Rv2615c to be an antigenic protein (Vaxijen score of 1.73). Homology and function-based characterization revealed high similarity of Rv2615c with APAF1-apoptosome and involvement in Cysteine-type endo-peptidase activation process during apoptotic pathway. To validate these *in-silico* results,*in-vitro* experiments with recombinant Rv2615c and THP-1 macrophages were conducted. Our results showed that Rv2615c protein of Mtb induced host macrophage apoptosis and Caspase activation indicating that this protein might be employed by the pathogen during late stages of infection at the site of granuloma where it may facilitate disease persistence through apoptosis induction. During late stages of infection, the granuloma is maintained by activated macrophages. To understand the role of Rv2615c in macrophage activation and granuloma maintenance, we probed the expression of TLRs, HLA-DR, NF-B and pro-inflammatory cytokines. Experiments with Rv2615c-stimulated THP-1 macrophages showed up-regulated levels of TLR4-MyD88, antigen presenting HLA-DR molecules, NF-B and inflammatory TNF-α cytokine. To get further insight into the apoptotic function of Rv2615c, a thorough sequence scan was done which highlighted the presence of eukaryotic CARD (Caspase Activation and Recruitment Domains)-like domain in Rv2615c similar to CARD domains in Apoptotic Peptidase Activating Factor 1 (APAF1) and Caspase9. Docking and Molecular Dynamic (MD) simulation studies substantiated the high binding stability of Rv2615c complex with CARD-APAF1 and CARD-Caspase9. Two critical residues (Leu116 and Ile117) in the CARD-like domain of Rv2615c was found to be either conserved or highly similar and aligned with the conserved residues of APAF1-CARD and Caspase9-CARD domain. Docking and MD simulation studies confirmed that the mutation and deletion of these two residues decreased the stability of Rv2615c protein and its affinity to bind CARD domain of APAF1 and Caspase9. Validation through site-directed mutagenesis experiments will give further insight of molecular mimicry adopted by Rv2615c protein of Mtb.

2. RESULTS:

2.1 *In-silico* characterization of Rv2615c

2.1.1 Rv2615c is an antigenic protein predicted to be involved in host cell death pathways

Vaxijen 2.0 server predicted Rv2615c to be a probable antigen with high score of 1.73. 5 models were generated for secondary structure prediction using I-TASSER server which were further subjected for energy minimization in Chiron server. Model 1 was selected based on the C score of -3.06 in I-TASSER. Ramachandran plot for Model 1 showed 97.5% residues were present in favoured and generously allowed region while only 2.5% residues were present in disallowed region. Errat score was 86.67 for Model 1 and Verify3D score was 81.13.

I-TASSER predictions related to functional role strongly pointed the involvement of Rv2615c in host cell death pathways. Three top predicted structural analogs and Gene ontology templates for Rv2615c were those of Apoptosome complex (PDB ID: 5JUL, 3IZ8, 1VT4) and Apoptosome-ProCaspase9 CARD complex (PDB ID: 3IYT, 3IZA). Consensus GO terms for biological process and molecular functions were – GO: 0006917 (apoptotic process) and GO: 006919, GO: 0043028, GO: 0016505 (apoptotic process involved in activation of cysteine type endo-peptidase activity).

2.2 In vitro assessment of Rv2615c for inducing apoptosis

3.2.1 Cloning, expression and purification of recombinant Rv2615c protein

His-tagged recombinant Rv2615c protein was successful with pGEMT easy vector in DH5α followed by pET28a[+] expression vector in BL21*DE3* and the clones were also confirmed by sequencing. Rv2615c was successfully expressed and purified from insoluble fraction of transformed BL21 *DE3* culture by affinity chromatography. The protein had a molecular weight of 39.3 kDa observed in SDS-PAGE and anti-His antibody on western blotting (Fig S1). One liter of culture yielded approximately 2 mg/mL of protein. The purified protein was passed through polymyxin B-agarose beads to remove bacterial endotoxin and Limulus Amoebocyte Lysate assay (Pierce, USA) was performed in collected fractions which confirmed no endotoxin contamination.

2.2.2 (a) Rv2615c protein induces cell death in THP-1 macrophages

To determine the cell viability, MTT and CellTiter Blue assay were performed to probe any change in viability of THP-1 cells in response to Rv2615c stimulation. Three concentrations of Rv2615c (5μg/ml, 10μg/ml and 15μ/ml) were included for checking the dose dependent viability. Cell viability was prominently affected in Rv2615c stimulated cells in a dose dependent manner (Fig S2a). Based on these observations, we selected 10μg/ml as stimulation concentration for Rv2615c protein in our experiments. Unless otherwise stated, LPS and staurosporine served as controls in each experiment. Viability of Rv2615c-stimulated and control-stimulated THP-1 macrophages was significantly decreased at all-time points when compared to unstimulated cells (Fig S2b and S2c). In comparison to the unstimulated cells, Rv2615c-stimulation caused approximately 50 to 60% cell death till 48 hours that was comparable to cell death induced by LPS stimulation (Fig S2b and S2c). These observations indicate that Rv2615c protein affects viability and induce cell death in THP-1 macrophages.

2.2.2. (b) Rv2615c protein did not induce LDH, a marker for the necrotic cell death

LDH release usually determines the cellular cytotoxicity in response to external stimulus; moreover, it also defines if the cells are undergoing necrotic cell death. 1% Triton-X, lysis buffer and a positive control was included as controls in study. Rv2615c-stimulation led release of LDH was observed to be at basal level, comparable to the unstimulated cells (Fig S3). Levels of LDH were significantly high in each of the positive controls included in the study at 16h, 24h and 48h. These observations indicate that the cell death induced by Rv2615c protein is not necrosis.

2.2.2. (c) Rv2615c-stimulation leads to flipping of phosphatidylserine on outer membrane and apoptosis of THP-1 macrophages

Phosphatidylserine [PS] is flipped from the inner to the outer leaflet of the plasma membrane as a result of biochemical alterations associated with the initiation of apoptotic pathway. Rv2615c-stimulation showed

an increase in early apoptosis indicated by annexinV positive cells (Fig 1b, bottom right quadrant) plus late apoptosis indicated by annexinV/PI dual-positive cell population (Fig 1b, top right quadrant) in a time-dependent manner. At 16h, there was no significant increase in percentage of both the cell populations (early apoptotic annexinV positive; late apoptotic annexinV/PI positive cells) on stimulation with Rv2615c protein as compared to unstimulated control (Fig 1a). At 24h and 48h, Rv2615c-stimulation showed gradual and significant increase in percentage of dual positive cell populations (Mean±SEM in range of 37 to 49%) as compared to unstimulated cells (Mean±SEM in range of 27 to 35%) while the cell death was comparable to LPS stimulation (Mean±SEM range of 33 to 47%) at 48h. Since Staurosporine is a well-known cell death inducer; we observed maximum cell death (Mean±SEM value of 62%) till 48h (Fig 1a).

2.2.2 (d) Rv2615c stimulation leads to DNA fragmentation in THP-1 macrophages

DNA fragmentation is another distinct feature of cells undergoing apoptosis which was studied by TUNEL assay. At 16h, 24h and 48h, the percentage of TUNEL positive cells in response to Rv2615c-stimulation (Mean±SEM range of 22 % to 35%) were significant than the unstimulated cells (Mean±SEM range of 3 % to 25%) and comparable to positive control (LPS/Staurosporine stimulated) cells (Fig 1c and 1d). These results depicted that the putative Rv2615c protein induces apoptotic cell death in THP-1 macrophages.

2.2.2 (e) Rv2615c protein trigger the activation of Caspase9 in THP-1 macrophages

Initiator Caspase 9 activation is necessary for the development of the apoptosome complex and the subsequent activation of executioner Caspases 3 and 7, which results in apoptotic cell death. To check the engagement of initiator Caspase9 with respect to apoptosis induction by selected recombinant protein, western blot assessment of the total cell lysate from THP-1 macrophages post-stimulation with Rv2615c protein was done to determine if initiator Caspase9 was activated for the induction of apoptosis in response to Rv2615c. Levels of activated Caspase9 was quantified using ImageJ and revealed to be increased in response to Rv2615c stimulation relative to unstimulated cells and LPS stimulation (Fig 2a and 2b).

2.2.2. (f) Rv2615c-induced apoptotic cell death involves activation of Caspase 3 and 7

Classical intrinsic apoptosis includes the activation of Caspase 3 and Caspase 7 as the ultimate executioner caspases following APAF1-Caspase9-apoptosome formation. As a result, we investigated the activation of Caspase 3 and Caspase 7 during Rv2615c-mediated cell death. Rv2615c protein leads to activation of Caspase 3 and 7 at all the time points shown by significant increase in the percentage of Caspase 3 and 7 positive cells (Fig 2c). Rv2615c-stimulation led to a significant 1.5-fold increase in Caspase 3 and 7 activations than unstimulated cells. Staurosporine and LPS included as positive controls in the study led to approximately 1.6-fold increase in percentage of Caspase 3 and 7 positive cells than the unstimulated cells at 48h. The percentage of Caspase 3 and 7 positive cells was decreased by approximately 1.5 folds when pre-treated with pan caspase inhibitor Z-VAD-fmk in cells stimulated with Rv2615c protein and controls at 24h (Fig 2d). Additionally, the percentage of AnnexinV/AnnexinV-PI dual positive cells stimulated with Rv2615c protein decreased by 1.3-fold when pre-treated with pan Caspase inhibitor Z-VAD-fmk at 24h (Fig 2e). These results depicted that the selected Rv2615c protein induces Caspase 3 and 7 dependent apoptotic cell death in THP-1 macrophages.

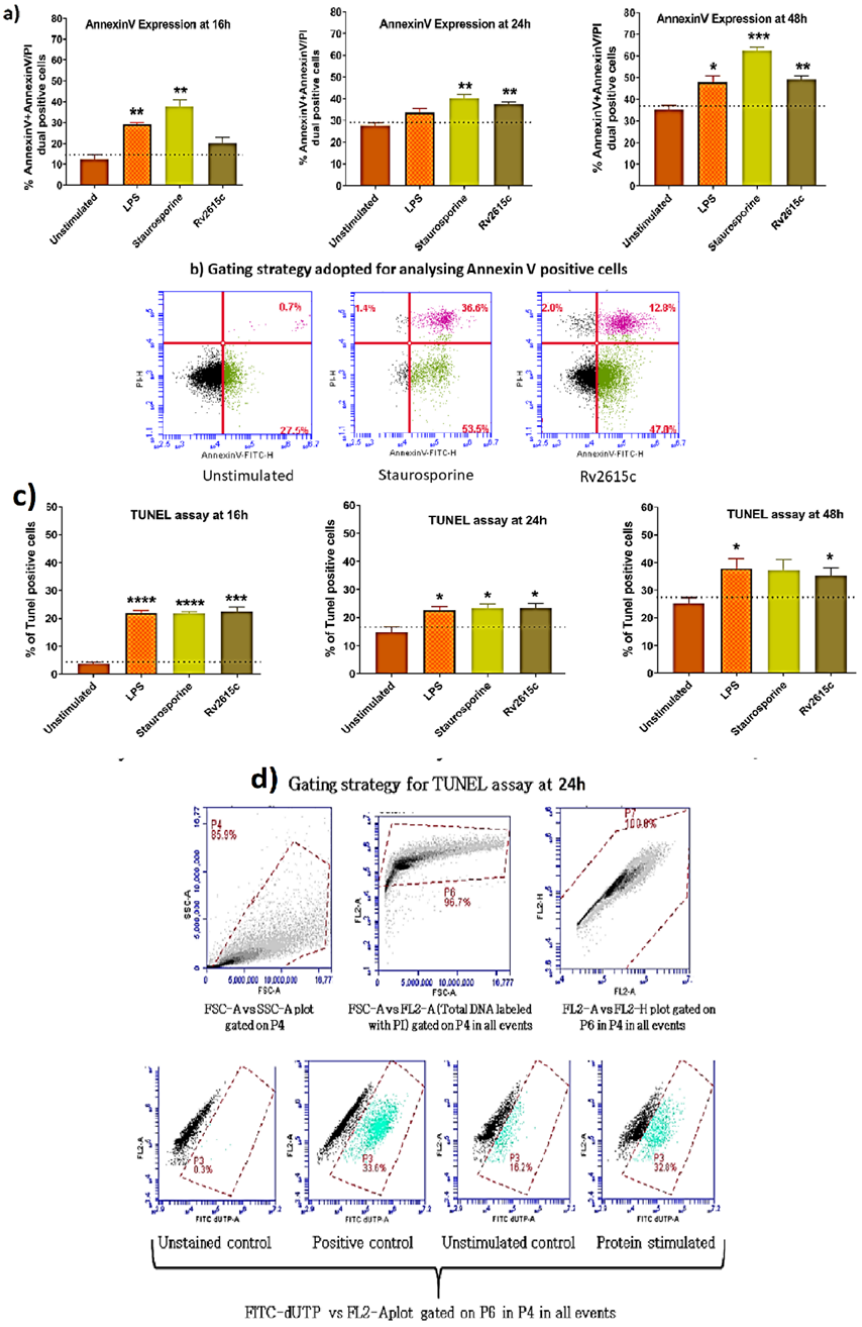

Figure 1. Flow cytometry analysis of AnnexinV and TUNEL positive cells expression in THP-1 macrophages following protein stimulation at different time points

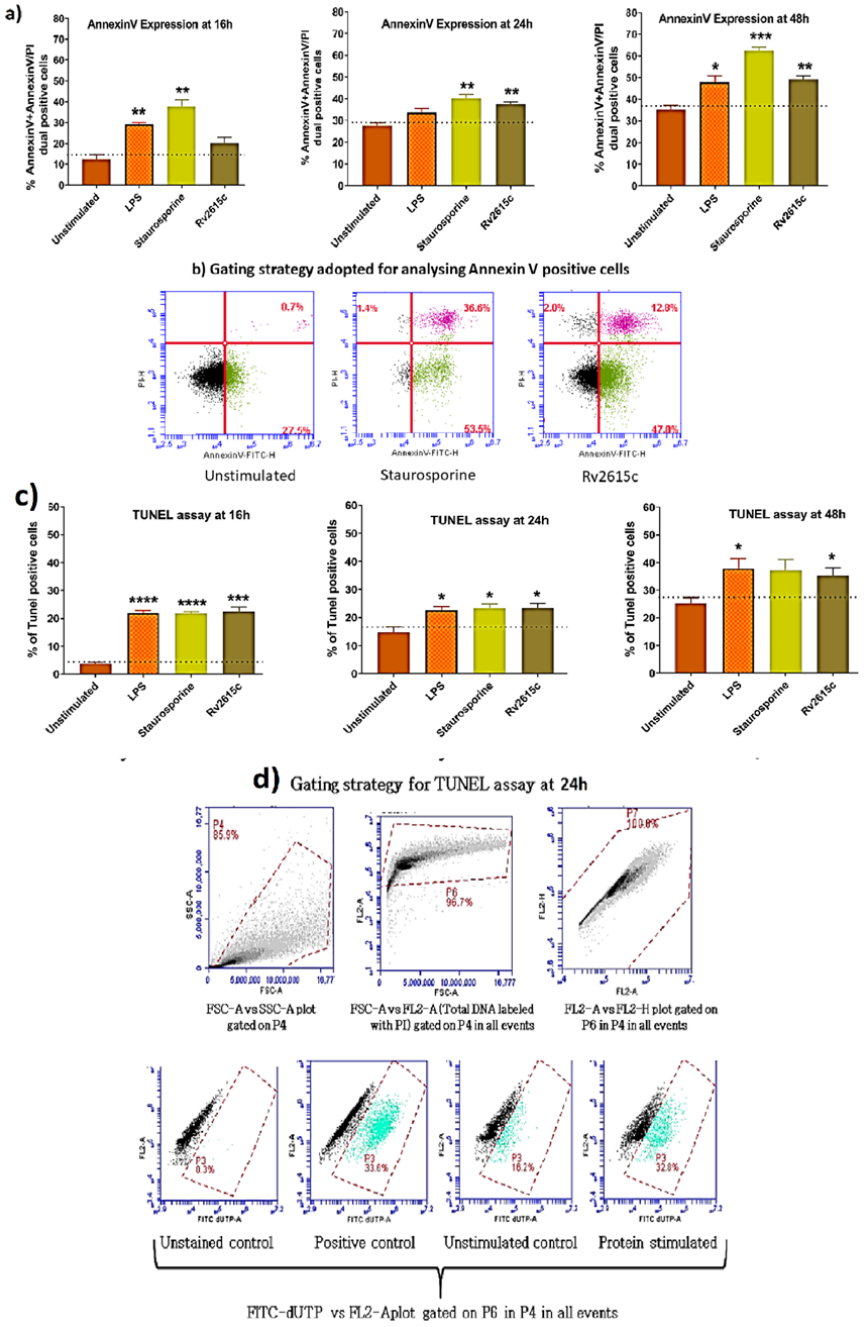

THP-1 macrophages were left unstimulated or stimulated with control/Rv2615c protein for 16h, 24h and 48h. Annexin V-FITC and PI/ TUNEL assay was performed in Flow Cytometer. 1(a) Graphs were plotted for different time points with a) % of annexinV + annexinV/PI dual positive cells and c) % of TUNEL positive cells on y axis and control/Rv2615c protein on x axis. Statistical analysis was done with Student's t test and results are Mean ± SEM of three independent experiments where * represents comparison with unstimulated cells and *P<0.05, **P<0.01, ***P<0.001, ****P<0.0001. 1(b) Dot plot showing gating strategy for cells stained with AnnexinV-FITC and PI staining which were analysed by Flow Cytometer. Plots were generated as annexinV fluorescence (FL1) on x axis and PI fluorescence (FL3) on y axis. Total 10000 events were

acquired for each sample and threshold was set at 80000. Cells in lower right quadrant coloured in green depicts percentage of annexinV single positive (early apoptotic cells); cells in upper right quadrant colours in red depicts percentage of annexinV /PI dual positive (late apoptotic cells); cells in upper left quadrant depicts percentage of PI single positive (necrotic cells). 1d) Dot plot showing gating strategy for percentage of TUNEL positive cells following staining with FITC-dUTP and PI to label the DNA breaks. Plots were generated as FITC-dUTP (FL1) on x axis and PI fluorescence (FL2) on y axis. Total 10000 events were acquired for each sample and threshold was set at 80000. Cells in gate P3 shows the total percentage of TUNEL positive cells or cells with DNA breaks.

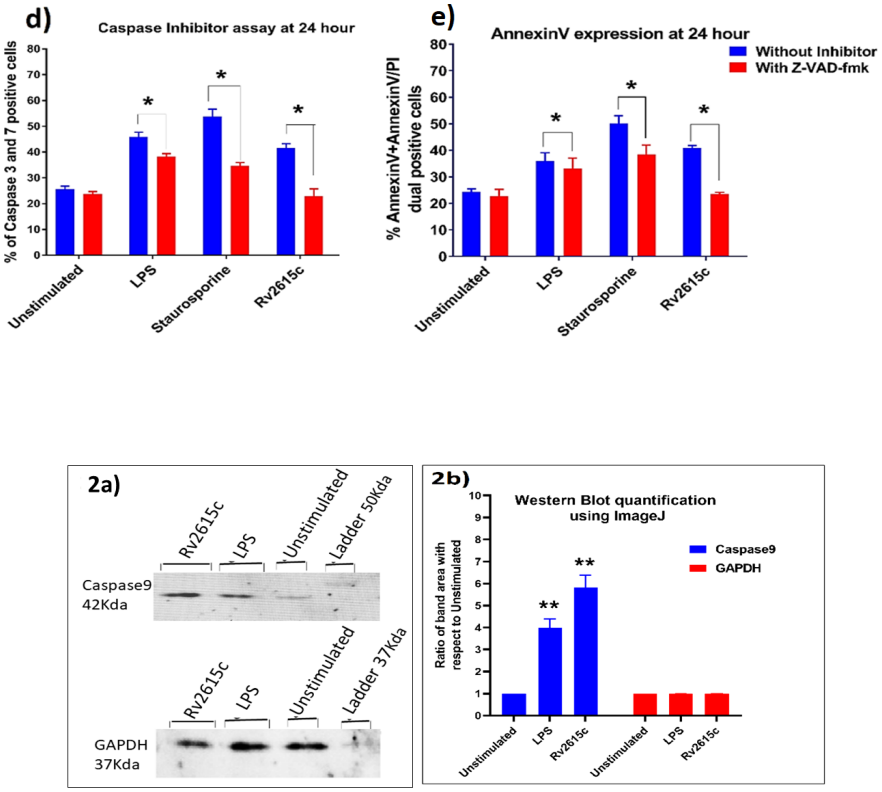

Figure 2. Western blot and graphs depicting activation of Caspase9 and Caspase 3 and 7 respectively following protein stimulation of THP-1 macrophages

Activated Caspase9, 3 and 7 estimation experiments were carried out on THP-1 macrophages that had either been left unstimulated or stimulated with control/Rv2615c protein. (a) Western blot image showing bands for activated Caspase9. Proteins were transferred onto the PVDF membrane after cell lysate was prepared and separated on SDS-PAGE post 24 hours stimulation. The polyclonal anti-Caspase9 antibody was used to measure the amounts of activated Caspase9, and an internal loading control, GAPDH, was employed at a dilution of 1:1000. b) ImageJ software was used to quantify the size of each western blot band. Results are shown as the meanSEM values of three separate experiments and were examined by showing the ratio of each band area with respect to unstimulated cells. Student's t test was performed where * depicts the comparison with unstimulated cells for Caspase9 and GAPDH separately. (*P<0.05, **P<0.01). c) Unstimulated/control/Rv2615c protein stimulated THP-1 macrophages were incubated for different time

points (16h, 24h and 48h) and activation of Caspase 3 and 7 was estimated which is a characteristic of intrinsic apoptosis.

Each western blot band was measured using ImageJ software. The ratio of each band area with respect to unstimulated cells was investigated, and the results are presented as them Mean±SEM values of three distinct experiments. The comparison of Caspase9 and GAPDH individually with unstimulated cells was shown using the Student's t test, where *. (*P<0.05, **P<0.01). c) THP-1 macrophages that were left unstimulated or stimulated with control/Rv2615c protein were incubated for different time points (16 hours, 24 hours, and 48 hours), and the activation of caspase 3 and 7 was estimated. THP-1 cells were also blocked with z-VAD-fmk Caspase inhibitor prior to stimulation and evaluated for d) levels of Caspases 3 and 7 and e) expression of AnnexinV/AnnexinV-PI dual positive cell population at 24h. Graphs were plotted for different time points with % of positive cells on y axis and control/Rv2615c on x axis. Statistical analysis was done with Student's t test and results are Mean ± SEM of three independent experiments where * represents comparison with unstimulated cells and *P<0.05, **P<0.01, ***P<0.001.

2.3. Rv2615c protein enhances the expression of TLR4, HLA-DR and downstream effector molecules to modulate the host immune response

2.3. (a) Docking studies revealed preferential binding of Rv2615c protein with TLR4 than TLR2

TLRs in particular are essential for the recognition of the pathogenic Mtb proteins. The interaction of PE_-PGRS proteins with TLRs has been shown in a number of studies (Abdallah *et al.* , 2007; Bansal*et al.* , 2010; Ramakrishnan, 2012; Grover *et al.* , 2018; Liu*et al.* , 2020). I-TASSER homology modelled Rv2615c protein docking experiments with TLR2 and TLR4 demonstrated Rv2615c's strong affinity for TLR4 binding (Fig 3a). HADDOCK predicted a score of -141.3±13.8 for Rv2615c-TLR4 docked complex while -109.5±5.8 for Rv2615c-TLR2 docked complex. The TLR2-Rv2615c complex had a total of 46 structures, which were grouped into 9 clusters, whereas the TLR4-Rv2615c complex had 67 structures, which were grouped into 9 clusters. TLR2 and Rv2615c complexes were predicted to have the best Z scores, with -2 for TLR2 and -1.7 for Rv2615c.

2.3. (b) Rv2615c leads to up-regulation of TLR4 and HLA-DR expression

Expression profile of TLR2 and TLR4 was estimated by flow cytometry in response to Rv2615c-stimulation in THP-1 macrophages. Both Rv2615c and LPS-a TLR4 agonist resulted in significant 1.27-fold increase in TLR4 percent positive cells at 24h than unstimulated control. There was no up-regulation of TLR4 expression observed for cells stimulated with cell wall fraction of Mtb. When THP-1 cells were blocked with Anti-TLR4 antibody prior to stimulation with Rv2615c or controls; the percentage of TLR4 positive cells significantly decreased by 1.4-fold implicating that the function of Rv2615c is TLR4 mediated. Further, there was no up-regulation in TLR2 expression in response to both LPS and Rv2615c-stimulation at all-time points. Cell wall fraction which was included as positive control for TLR2 expression showed a significant 1.2-fold increase in TLR2 expression at all-time points (Fig 3b).

For determining the effect of Rv2615c-stimulation on TLR-associated antigen presenting molecule HLA-DR, we performed flow cytometry analysis to study the expression of HLA-DR. Rv2615c showed significant increase in percentage of HLA-DR positive cells at 24h and 48h. At 24h, there was significant 2-fold increase in percentage of HLA DR positive cells induced by Rv2615c in comparison to unstimulated cells (Fig 3b).

In comparison to unstimulated cells, LPS and CWF significantly (˜1.5-fold) raised the levels of HLA-DR positive cells. We examined the HLA-DR levels in cells inhibited with anti-TLR4 antibody prior to stimulation to determine the TLR4-dependent up-regulation of Rv2615c-induced HLA-DR expression. In comparison to unstimulated cells, we observed a 2.8-fold decrease in HLA-DR expression in control (LPS and CWF) and Rv2615c-stimulated THP-1 macrophages (Fig 3c and 3d).

2.3. (c) Rv2615c leads to up-regulation of downstream effector molecule- MyD88 and NF-B

RT-PCR evaluation of cDNA from isolated mRNA of unstimulated and Rv2615c protein/LPS stimulated THP-1 macrophages revealed an increase in fold change in MyD88 gene expression after 24h of stimulation and in NF-B gene expression after 24 hours and 48 hours of stimulation. When compared to unstimulated cells, Rv2615c protein stimulation led to approximately ˜2.6-fold increase and LPS stimulation led to approximately ˜3-fold increase in the expression of MyD88 gene respectively (Fig 3d). Expression of NFκB was observed to be approximately ˜4-fold increase in response to Rv2615c and approximately ˜2 to 4-fold increase in response to LPS after 24 and 48hrs of stimulation as compared to unstimulated cells (Fig 3e).

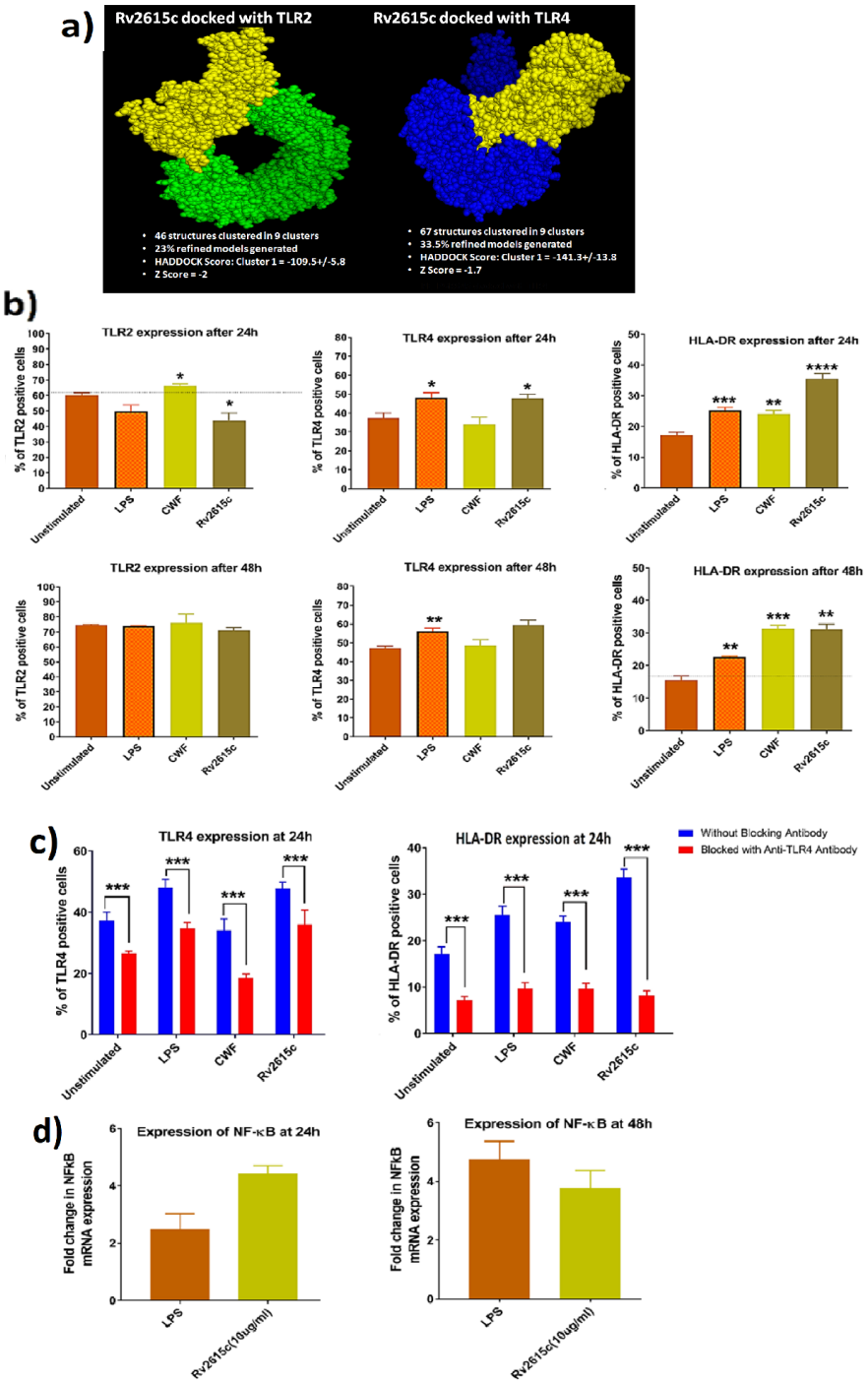

Figure 3. Expression profile of TLRs, HLA-DR, MyD88 and NF-B in Rv2615c-stimulated THP-1 macrophages

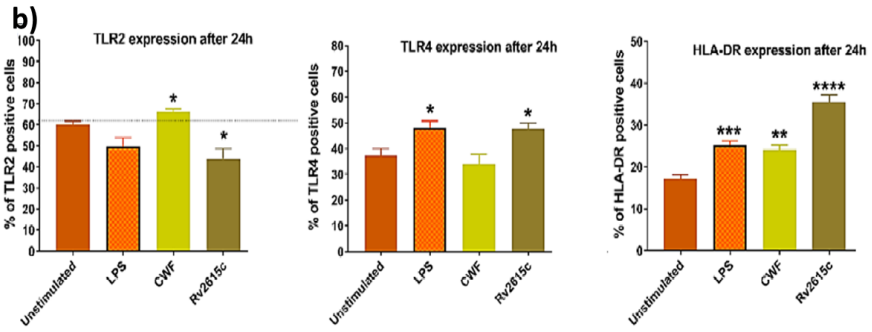

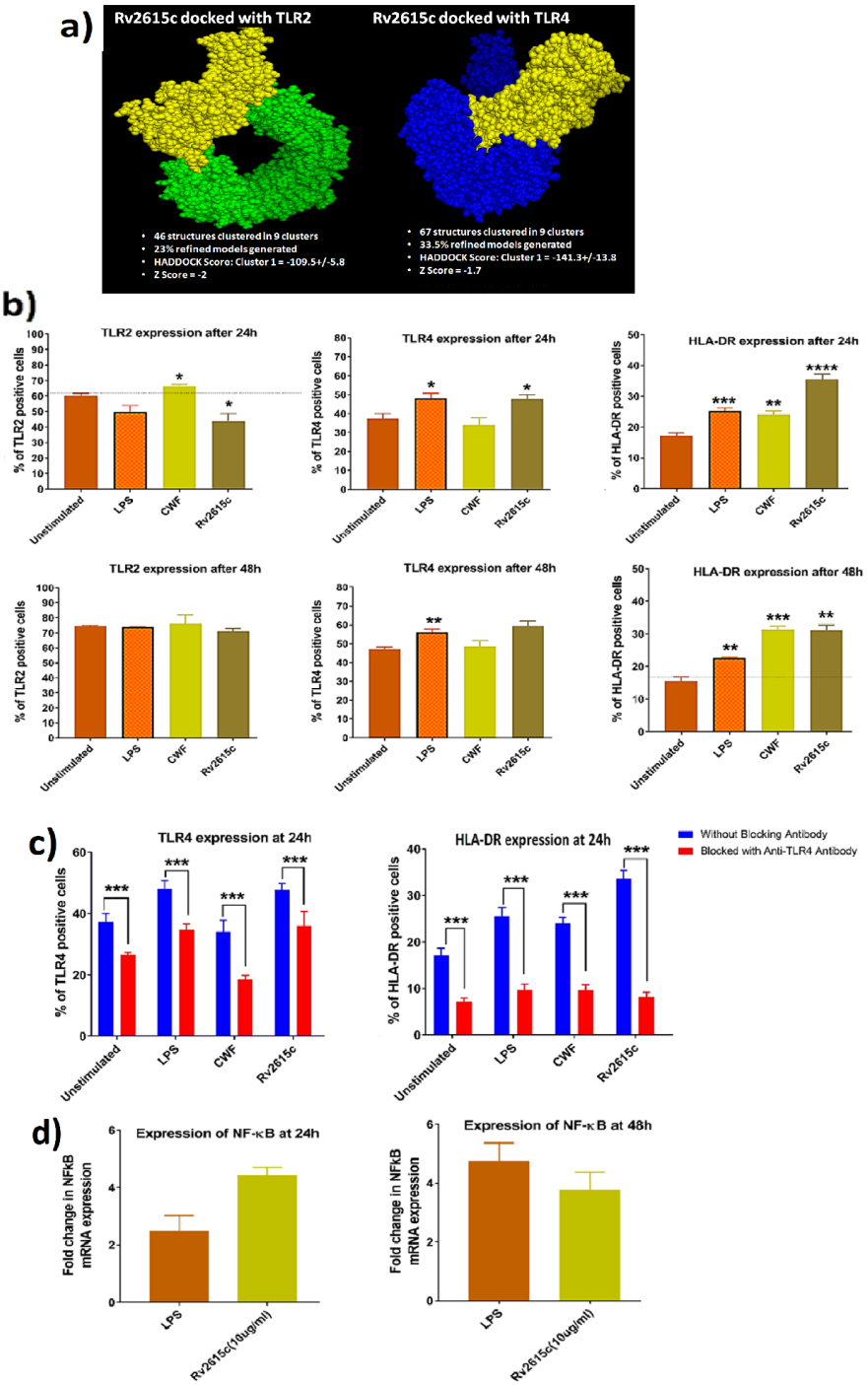

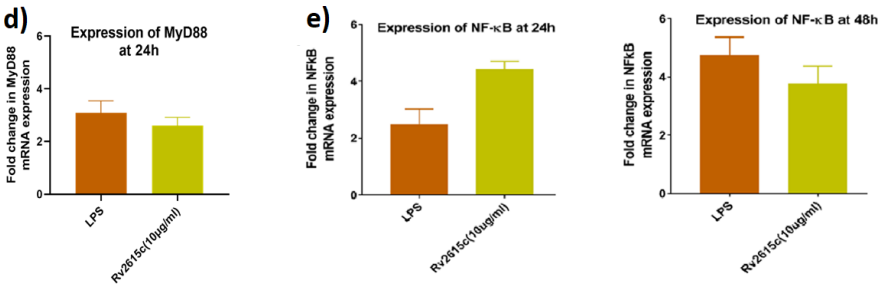

a) Predicted docked complex of Rv2615c (yellow) bound to TLR2 (green) and TLR4 (blue) using HADDOCK server. b) THP-1 macrophages were stimulated with control/Rv2615c protein for 24h and 48h. Expression profile of TLR2, TLR4 and HLA-DR was evaluated at 24h and 48h of stimulation. The percentage of TLR/HLA-DR positive cells was plotted on the y axis and control/Rv2615c protein on the x axis of graphs for various time points. The findings of the statistical study, which used the Student's t test, are shown as Mean±SEM for three separate experiments where * represents comparison with unstimulated cells and *P<0.05, **P<0.01, ***P<0.001. c) THP-1 cells were blocked with Anti-TLR4 antibody prior to stimulation and evaluated for levels of TLR4 and HLA-DR at 24h. Isolated mRNA from unstimulated or Rv2615c/LPS stimulated macrophages were synthesized into cDNA and RT-PCR was performed to estimate the levels of d) MyD88 and e) NF-κB gene expression using $2^{-[?][?]}$ CT method. MyD88 and NF-κB gene expression in unstimulated cells was considered 1 and with respect to unstimulated cells fold change in MyD88 and NF-κB gene expression in LPS and Rv2615c was plotted. Graphs were plotted for different time points with fold change in MyD88/NF-κB expression on y axis and LPS/Rv2615c protein on x axis. Results are expressed as Mean ± SEM of three independent experiments.

2.3 (δ) P2615ς λεαδς το υπ-ρεγυλατιον οφ προ-ινφλαμματορψ ςψτοκινε TNΦ-α βυτ δοων-ρεγυλατιον οφ IΛ-1β

A plethora of pro-inflammatory cytokines are secreted when an immune response is triggered. Additionally, pro-inflammatory immune response activation is also involved in various cell death mechanisms that take place at the host-pathogen interface. TLR4-NF-B signaling is a widely studied cascade known to activate key pro-inflammatory cytokines such as TNF-α. We found significantly up-regulated levels of TNF-α at all the time points in response to LPS and Rv2615c protein stimulated THP-1 macrophages as compared to unstimulated cells (Fig 4a). Both Rv2615c and LPS showed approximately ˜ 3 to 4-fold increase in TNF-α expression till 48h of stimulation. Another pro-inflammatory cytokine, IL-1β, is also reported to be released as a result of TLR4-NF-B signalling. IL-1 β is a modulator of extrinsic apoptosis via Caspase 8 activation and inflammasome activation. Interestingly, IL-1β levels in Rv2615c-stimulated macrophages were either equivalent to or lower than in unstimulated cells at all time periods. (Fig 4b). IL-1β expression in response to LPS stimulation was found to be significantly 2 to 3-fold up-regulated than unstimulated cells till 24h.

To further ensure that the release of TNF-α in response to Rv2615c protein stimulation was mediated by TLR4; we evaluated the expression of TNF-α after blocking the expression of TLR4. There was a 2-fold decrease in TNF-α release in response to Rv2615c and control stimulated THP-1 macrophages when blocked with Anti-TLR4 antibody prior to stimulation (Fig 4c).

Φιγυρε 4. ˜ψτοκινε ΕΛΙΣΑ το δετερμινε τηε λεελς οφ προ-ινφλαμματορψ ςψτοκινεσ-TNΦ-α ανδ IΛ-1β

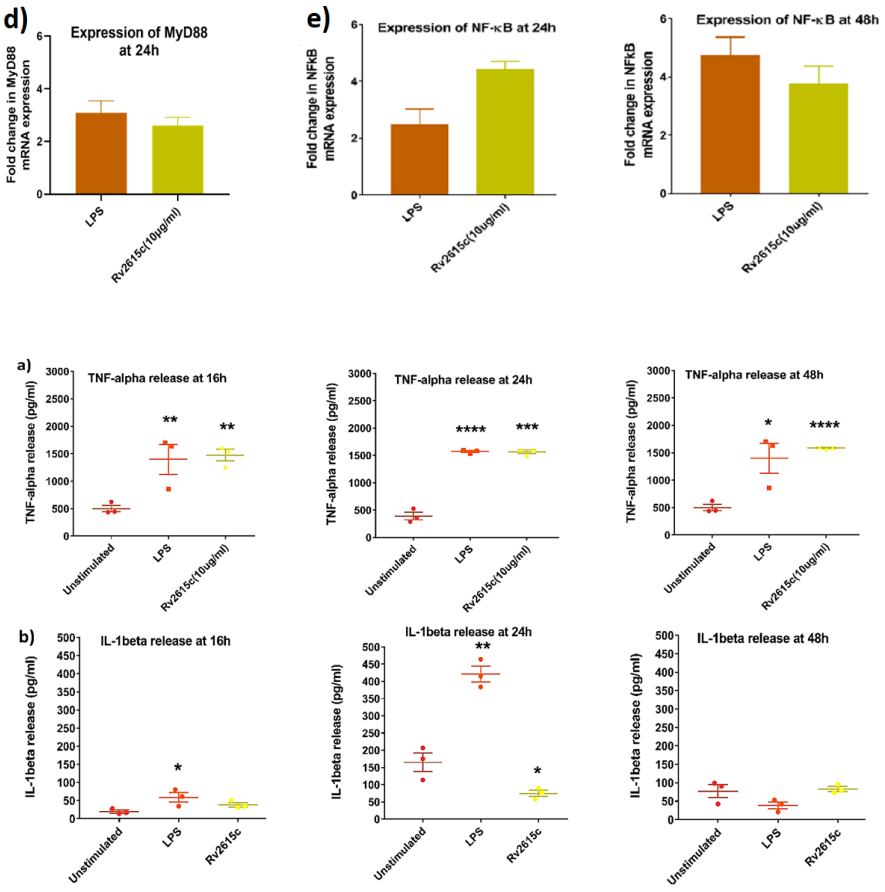

THP-1 macrophages were unstimulated or stimulated with LPS/Rv2615c protein and for 16h, 24h and 48h were analysed for release of a) TNF-α and b) IL-1β in cell culture supernatants c) TNF-α release was also estimated in supernatant blocked with Anti-TLR4 antibody prior to stimulation. ELISA was done according to manufacturer's instructions. Graphs were plotted for different time points with cytokine release in pg/ml on y axis, controls, and the protein Rv2615c on the x axis. The findings of the statistical analysis, which used the Student's t test, are shown as Mean ± SEM for three separate experiments where * represents comparison with unstimulated cells and *P<0.05, **P<0.01, ***P<0.001.

2.4 Rv2615c has CARD-like domain similar to CARD domains in APAF1 and Caspase9

In-silico clues pointed the similarity of Rv2615c protein with apoptosome complex and prediction of molecular function in activation of cysteine-type endopeptidase/Caspases during apoptosis. In-vitro studies substantiated the role of Rv2615c protein in inducing Caspase-mediated host macrophage apoptosis. APAF1-Apoptosome complex initiates the activation of Caspase9 and active Caspase9 is recruited via its CARD domain onto the CARD domain of APAF1. Our findings of Rv2615c led us to hypothesize- whether Rv2615c possess a CARD-like domain similar to CARD domains present in APAF1 and Caspase9 that facilitates interaction and activation of cysteine type endo-peptidase activity of Caspase9. Multiple sequence alignment of Rv2615c protein with CARD domains of APAF1 and Caspase9 revealed many conserved and highly similar amino acid residues (Fig 5b and 5c). CARD domains of both APAF1 and Caspase9 are known to contain some highly conserved mostly hydrophobic and crucial residues through which protein-protein interactions occur (Fig 5a). We observed 14 crucial residues of APAF1-CARD and 9 crucial residues of Caspase9-CARD either totally conserved or highly similar in Rv2615c protein positioned from 60 to 230 amino acids which we denoted as CARD-like domain (Fig 5b, 5c and S4a). Interestingly, the MINNOU server predicted that

the CARD-like domain in Rv2615c is mostly hydrophobic in nature similar to the CARD domains of APAF1 and Caspase9 (Fig S4b). The secondary structure characterization reveals that the CARD-like domain in Rv2615c contains highly disordered random coiled region and fewer alpha-helixes (Fig S4b). Structural superimposition showed helical region of CARD-like domain in Rv2615c mostly aligned with CARD-APAF1 and CARD-Caspase9 (Fig S5). Coiled regions are highly flexible and unstable which facilitate dynamic protein-protein interactions.

Figure 5. Multiple sequence alignment of CARD domains

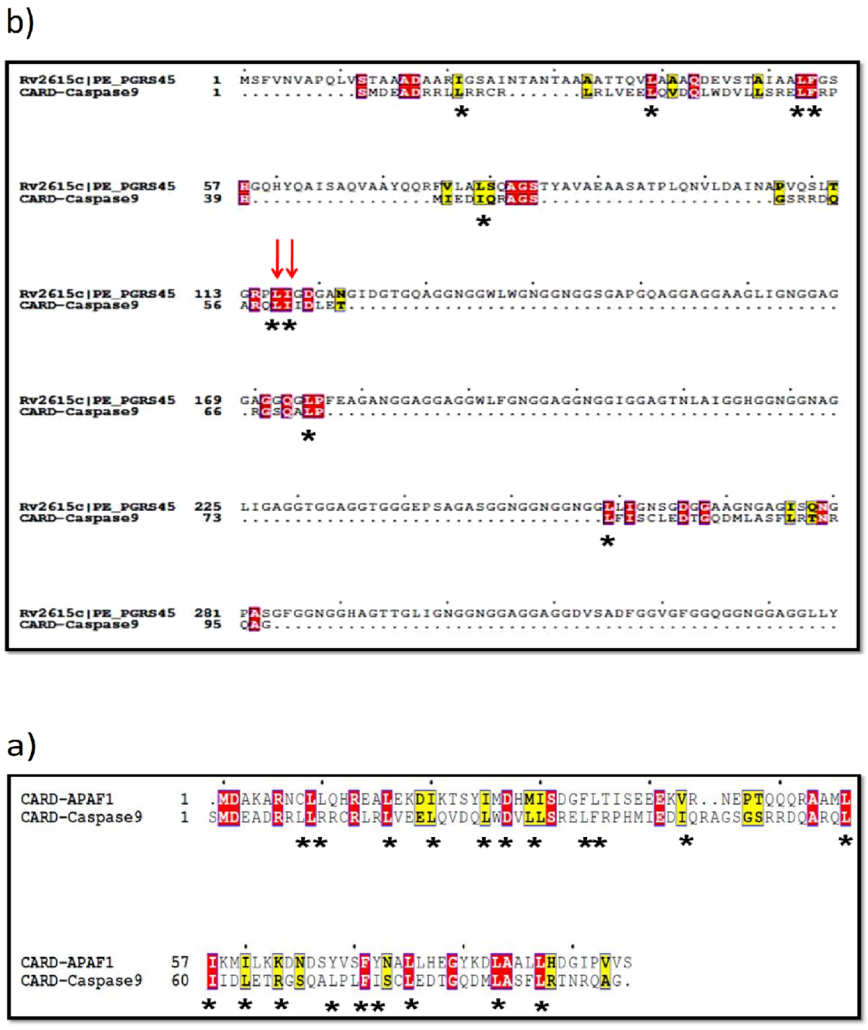

c)

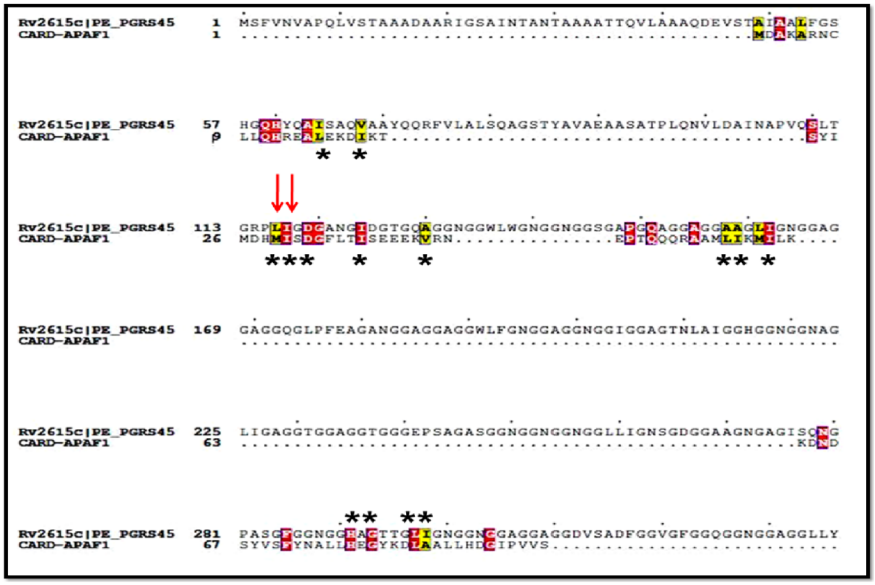

Multiple sequence alignment of 8(a) CARD-APAF1 and CARD-Caspase9 8(b) Rv2615c and CARD-Caspase9 8(c) Rv2615c and CARD-APAF1. All the crucial conserved or similar residues are denoted by asterisk (*). The common Leucine116 and Isoleucine117 residues in Rv2615c protein which were mutated to Alanine are denoted by red arrow.

2.4.1 CARD-like domain of Rv2615c has strong binding affinity for CARD domains of APAF1 and Caspase9

Docking studies with whole Rv2615c protein revealed that its CARD-like domain could bind strongly with CARD-APAF1 (Hex energy score: -655.54 Kcal/mol) and with CARD-Caspase9 (Hex energy score: -694.29 Kcal/mol) (Fig 6). Rv2615c formed 25 bonds (3 electrostatic, 7 hydrogen and 15 hydrophobic bonds) with CARD-APAF1 while 24 bonds (6 electrostatic, 6 hydrogen and 12 hydrophobic bonds) with CARD-Caspase9 through its CARD-like domain (Fig S6). These Hex energy scores were much higher than the Hex scores of positive controls included in the study i.e., complex of CARD-APAF1 with CARD-Caspase9 (PDB ID 3YGS- Hex score: -463.25 Kcal/mol) (Fig 6). However, Hex score for Rv2615c docked with APAF1-ADP was very less (-110.48 Kcal/mol) compared to the positive control. This could possibly be because of low affinity of Rv2615c for inactive form of APAF1 protein that is not bound to Apoptosome complex.

We observed two crucial adjacent hydrophobic residues i.e., Leucine-116 and Isoleucine-117 in CARD-like domain of Rv2615c which were common, totally conserved or similar and aligned with conserved residues of CARD-APAF1 (Methionine-29 and Isoleucine-30) and CARD-Caspase9 (Leucine-58 and Isoleucine-59). These residues (Leucine-116 and Isoleucine-117) within Rv2615c were also involved in bond formation with CARD-APAF1 and CARD-Caspase9 (Fig S6). Mutant of Rv2615c in which Leucine-116 and Isoleucine-117 within the CARD-like domain were mutated to Alanine was less stable. The binding affinity of this mutant Rv2615c with CARD-APAF1 and with CARD-Caspase9 was also decreased. Mutant Rv2615c protein bound to APAF1 CARD with energy score of 594.43 Kcal/mol and with Caspase9 CARD with energy score of -646.87 Kcal/mol.

2.1.4 Validation of docking results through MD simulation

The RMSD and RMSF plots obtained after the extensive (100 ns) MD simulation confirmed the structural stability of the protein-protein complexes (Fig 7). The RMSD value of backbone for all the complexes increased for initial 10 to 20ns following which it became stable with an average value of 1nm to

1.2nm for Rv2615c-APAF1 CARD and Rv2615c-Caspase9 CARD till 100ns. The RMSD value for mutant Rv2615c-APAF1 CARD was comparable to that of Rv2615c- APAF1 CARD while the RMSD value of mutant Rv2615c-Caspase9 CARD was higher in the range of 1.4nm. The average RMSD value of control structure was 0.70nm. RMSF analysis revealed that the docked complexes of Rv2615c protein with APAF1-CARD and Caspase9-CARD and mutant Rv2615c with Caspase9-CARD displayed average RMSF value of 0.80nm. Mutant Rv2615c with APAF1-CARD showed high fluctuations with average RMSF value in range of 1.20nm. The average RMSF value of control structure was 0.30nm. Overall, MD simulation results revealed that the docked complexes of Rv2615c showed a comparatively higher RMSD and RMSF value than control structure (APAF1-CARD with Caspase9-CARD) but all values are in acceptable range. One reason for this higher RMSD and RMSF values of Rv2615c docked structures could be large size of Rv2615c protein (461 residues) in comparison to the APAF1-CARD (95 residues) and Caspase9-CARD structures (97 residues).

Figure 6. Molecular docking of Rv2615c protein with CARD domains of APAF1 and Caspase9

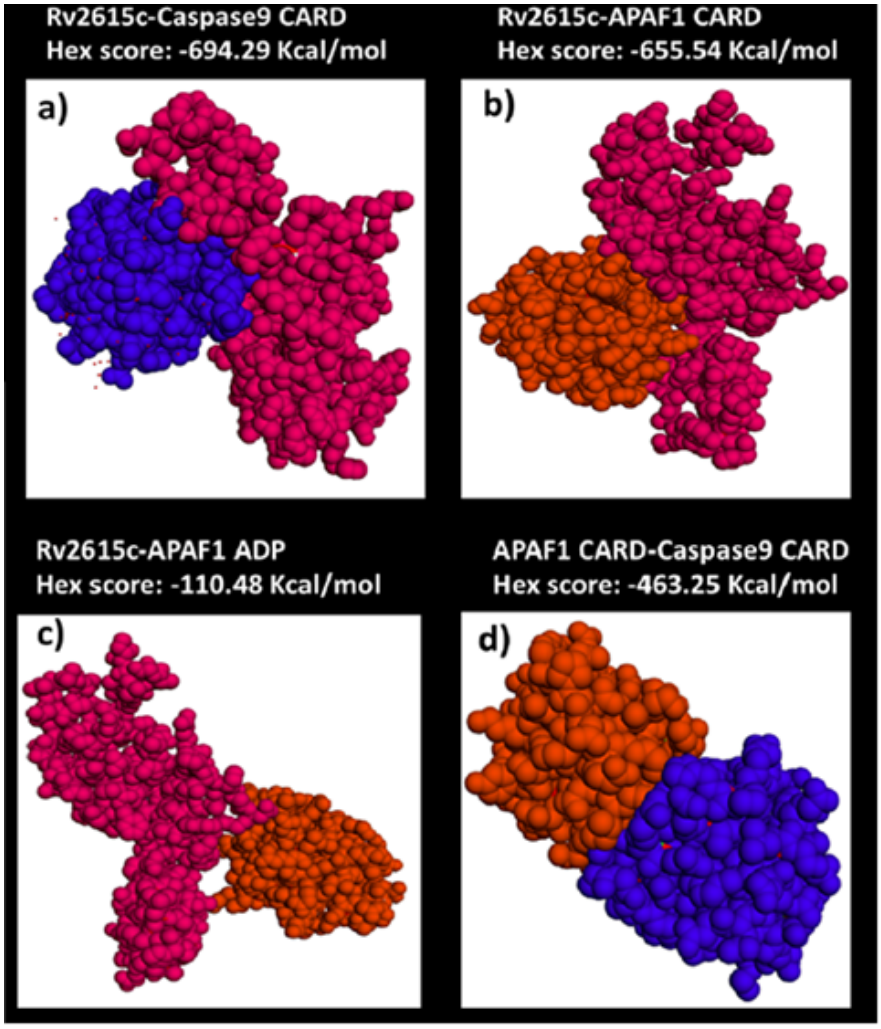

Rv2615c protein (pink color) showed high affinity for CARD domain of both APAF1 (orange color) and Caspase9 (blue color) and establishes interaction via its CARD-like domain. The binding affinity of Rv2615c for CARD domain of both APAF1 and Caspase9 was much higher than the positive control included in the study involving interaction of APAF1 CARD and Caspase9 CARD. However, Rv2615c showed low binding

affinity for inactive form of APAF1 ADP implicating its preference for active APAF1 Apoptosome complex.

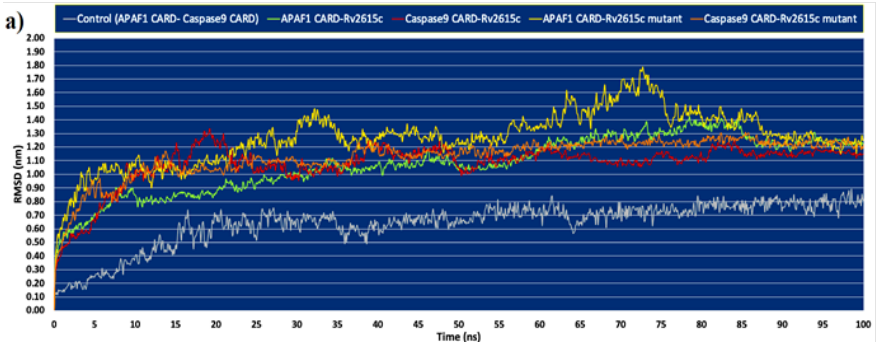

Figure 7. MD Simulation of docked structures

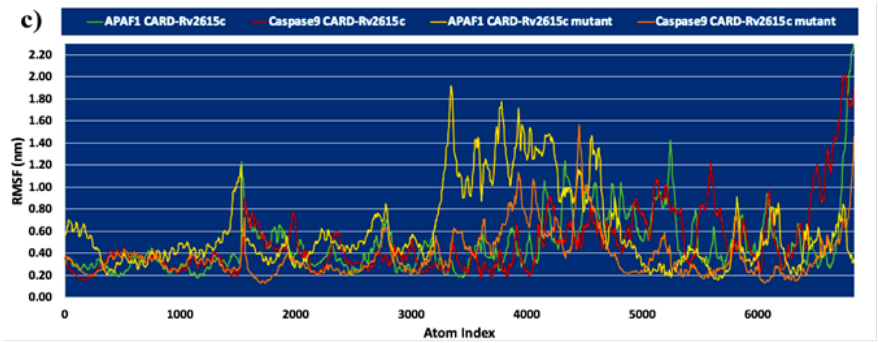

MD simulations for 100 ns was performed for Rv2615c protein docked with APAF1 CARD, Caspase9 CARD and mutant Rv2615c protein docked with APAF1 CARD, Caspase9 CARD. Docked complex of APAF1 CARD and Caspase9 CARD was included as positive (a) Root mean square deviation for complex backbone with x axis denoting time in ns and y axis denoting RMSD in nm (b) and (c) Root mean square fluctuation of backbone for control (APAF1 CARD and Caspase9 CARD) and other complexes with x axis denoting atom index of complex and y axis denoting RMSF in nm.

3. DISCUSSION

Mtb is one of the most successful pathogens that has evolved since decades to be able to evade the host mediated immune responses. Virulent Mtb possess the recently evolved PE_PGRS subfamily proteins which have been reported to be crucial in pathogenesis and immuno-modulation (Brennan, 2017). However, the specific function of only some of these PE_PGRS proteins have been investigated in Mtb pathogenesis.

One uncharacterized protein of the PE family is Rv2615c protein which has been reported to be upregulated during dormant TB infection. This study was conceived to investigate the possible role of PE_PGRS45 (Rv2615c) in host cell death and immune response modulation. I-TASSER based homology mapping showed similarity between Rv2615c and APAF1-Apoptosome complex. Additionally, functional and molecular Gene Ontology predictions showed possible role of Rv2615c protein in host cell death pathways particularly pinpointing its role in apoptosis and cysteine type endo-peptidase activation. To experimentally evaluate the role of this protein in host macrophage apoptosis, *in-vitro*experiments were performed with recombinant Rv2615c protein. Our results established that the Rv2615c protein reduces cell viability and induces apoptotic cell death in THP-1 macrophages as analysed through MTT and CellTiter Blue assay, Annexin V-FITC/PI staining and TUNEL assay. About 12 PE_PGRS proteins are known to be expressed at late stage (at 90

days in guinea pig lungs upon Mtb infection) and some of them like PE_PGRS5 and PE_PGRS17 are reported to induce host cell death (Kruh *et al.* , 2010), (Chen *et al.* , 2013)(Grover *et al.* , 2018) (Medha, Sharma and Sharma, 2021). PE_PGRS33, one of the first extensively studied protein of this subfamily is also a potent Caspase-mediated apoptotic inducer of infected macrophages, although the time of its expression is unknown (Basu *et al.* , 2007). Because Rv2615c has been documented to be upregulated during dormant Mtb infection, it may also be a late stage expressing protein of Mtb which induces host macrophage apoptosis (Urán Landaburu *et al.* , 2020).*In-silico* analysis predicted Rv2615c to be involved in the activation of cysteine type endo-peptidase and it was observed that recombinant Rv2615c protein activated initiator Caspase9 and executioner Caspases 3 and 7 in THP-1 macrophages. Inhibitor studies with Caspase inhibitor led to decrease in apoptosis of THP-1 macrophages which implicates that apoptosis induced by our protein is Caspase mediated. Our results corroborates with the study of Augenstreich *et al.,*where the Mtb-induced apoptosis was blocked by Caspase inhibitors (Augenstreich *et al.* , 2017). During chronic TB infection, pathogen employs battery of proteins that can facilitate its survival and spread in host. Based on our observations, we propose that Rv2615c is one protein that is expressed to induce macrophage apoptosis within the granulomatous lesion and help Mtb in expanding its niche.

The Pathogen Associated Molecular Patterns (PAMPs) within Mtb interact with host TLRs activate macrophages and modulate various cell processes such as apoptosis, induction of oxidative stress, antigen presentation etc,.(Bansal *et al.* , 2010; Grover *et al.* , 2018; Liu*et al.* , 2020). Our *in-silico* results revealed preferential binding of Rv2615c to TLR4 as compared to TLR2. It was observed that stimulation with Rv2615c led to an increase in expression of TLR4, adapter molecule MyD88 and NF-B in THP-1 macrophages. Although PE_PGRS proteins such as PE_PGRS17 and PE_PGRS33 are shown to induce host cell apoptosis via TLR2 dependent pathway (Basu *et al.* , 2007; Chen*et al.* , 2013); our observation of Rv2615c's interaction with TLR4 gets support from the recent studies where PE/PPE proteins such as PE_PGRS5, PE6 and PE9-PE10 protein complex were found to induce apoptosis via TLR4-mediated signalling (Tiwari, Ramakrishnan and Raghunand, 2015; Grover *et al.* , 2018; Sharma *et al.* , 2021; Medha, Priyanka, *et al.* , 2022). Both TLR2 and TLR4 are key regulators in inducing apoptosis of Mtb infected macrophages. Signalling via TLR4 is crucial for maintaining balance between apoptosis and necrosis in Mtb infected macrophages (Sánchez *et al.* , 2010). A PE/PPE family protein- PE13 functions by engagement of TLR4 mediated up-regulation of NF-B and implicated in modulation of the macrophage activation and apoptosis (Li *et al.* , 2016). The Toll/Interleukin-1 Receptor Homology (TIR) Domains mediate the intracellular TLR associated signal transduction. TIR domain-activated signalling induces the recruitment of other adaptor molecules such as MyD88, which in turn triggers the activation of downstream effectors NF-B (Horng *et al.* , 2002; Yamamoto *et al.* , 2002). Activation of TLR4-MyD88-NF-B cascade is also responsible for production of proinflammatory cytokines TNF-α and IL-1β (Yamamoto*et al.* , 2002; Amaral and Andrade, 2017). In our study, levels of soluble TNF-α were observed to be up-regulated in Rv2615c-stimulated macrophages whereas no significant release of IL-1β was observed. As a key pro-inflammatory cytokine, TNF- also plays a significant role in the development and maintenance of lung granulomas in advanced stages of infection (Dorhoi and Kaufmann, 2014). Activation of TLR4-MyD88-NF-B signalling and increased levels of pro-inflammatory cytokines are prerequisite for activation of macrophages (Saraav *et al.* , 2017). To keep the macrophages active and conducive for Mtb proliferation, bacilli modulates an endogenous host mechanism for the resolution of exacerbated inflammation (Próchnicki and Latz, 2017). IL-1β is a mediator of inflammasome activation and plethora of studies have reported its heterogenous regulation (Mishra *et al.* , 2010; Hackett *et al.* , 2020). The transcriptional regulation of IL-1β is not only limited to TLR4-NFκB axis but is also controlled by macrophage immune-metabolic responses (Gleeson *et al.* , 2016). Recent findings established that persistent Mtb infection of macrophages was associated with suppression of glycolysis and reduced production of IL-1β, despite upregulated TNF-α levels (Próchnicki and Latz, 2017). Therefore, our observation of selective pro-inflammatory cytokine secretion of only TNF-α in response to Rv2615c indicates its role as modulator of macrophage functions to ensure bacilli survival and multiplication.

Although few PE/PPE proteins such as PE_PGRS47 are known to down-regulate antigen presenting HLA-DR molecules (Saini *et al.* , 2016); we observed stimulation of macrophages with Rv2615c led to an increase in

HLA-DR expression. Inhibitor studies with anti-TLR4 blocking antibody showed down-regulation in HLA-DR and TNF-α expression which suggests that the macrophage activation in response to Rv2615c could be TLR4 mediated. Observations of selective release of pro-inflammatory cytokine TNF-α, macrophage activation and induction of macrophage apoptosis in response to Rv2615c indicate that this protein has role in maintenance of the granuloma, dissemination and persistence of Mtb (Fig 8).

Since, we observed that Rv2615c shares homology with APAF1-Apoptosome which is a multimeric protein adaptor complex responsible for activation of initiator Caspase9, sequence scan of Rv2615c was done which discovered the presence of CARD-like domain similar to CARD of eukaryotic APAF1 and Caspase9. Interaction between APAF1-CARD and Caspase9-CARD is indispensable for Caspase9 activation (Hu *et al.* , 2014). This shows that Rv2615c could bind Caspase9 and APAF1 through its eukaryote-like CARD domain and may enhance Caspase9 activation. We found two adjacently placed critical residues (Leu116 and Ile117) in the CARD-like domain of Rv2615c which are conserved or highly similar and aligned with the conserved residues of APAF1-CARD and Caspase9-CARD domain. Molecular docking and simulation studies confirmed that the mutation and deletion of these two residues decreased the stability of Rv2615c protein and its affinity for CARD domain of APAF1 and Caspase9. Pathogenic microorganisms have rapidly acquired mechanisms to escape the host surveillance system through co-evolution with host cells. They harbour proteins which can imitate the eukaryotic proteins in terms of sequence, homology, function or possessing a short linear motif (SLiMs) or domains- a mechanism termed as 'molecular mimicry'. Many intracellular bacterial pathogens demonstrate remarkable example of molecular mimicry such as Legionella, Coxiella, Mycobacterium, Helicobacter, Chlamydia, and Bacillus which have been reported to contain eukaryote-like proteins with prominent role in infection (Chmiela and Gonciarz, 2017) (Sonia *et al.* , 2021). Therefore, our results suggest that Rv2615c protein could be a molecular mimic of CARD domain of APAF-1 and Caspase9 orchestrating apoptotic cell death. Furthermore, the significance of this CARD-like domain in Rv2615c needs to be validated further through site directed mutagenesis studies.

In conclusion, activation of TLR4-MyD88-NF-B-TNF-α signalling cascade, up-regulation of HLA-DR molecules and apoptotic cell death of macrophages induced by Rv2615c implicate that this protein has potential to evoke moderate host immune response to recruit immune cells at the site of granuloma and facilitates pathogen persistence by cell to cell spread via apoptosis (Fig 8). The strategy of molecular mimicry adopted by Rv2615c protein of Mtb enhances our understanding of Mtb pathogenesis and needs to be explored experimentally. Further investigations focused on Rv2615c may help in development of new TB therapeutics. Especially the use of inhibitors of apoptosis in dormant stages of TB infection could be a novel approach to prevent the spread of Mtb to new sites within host.

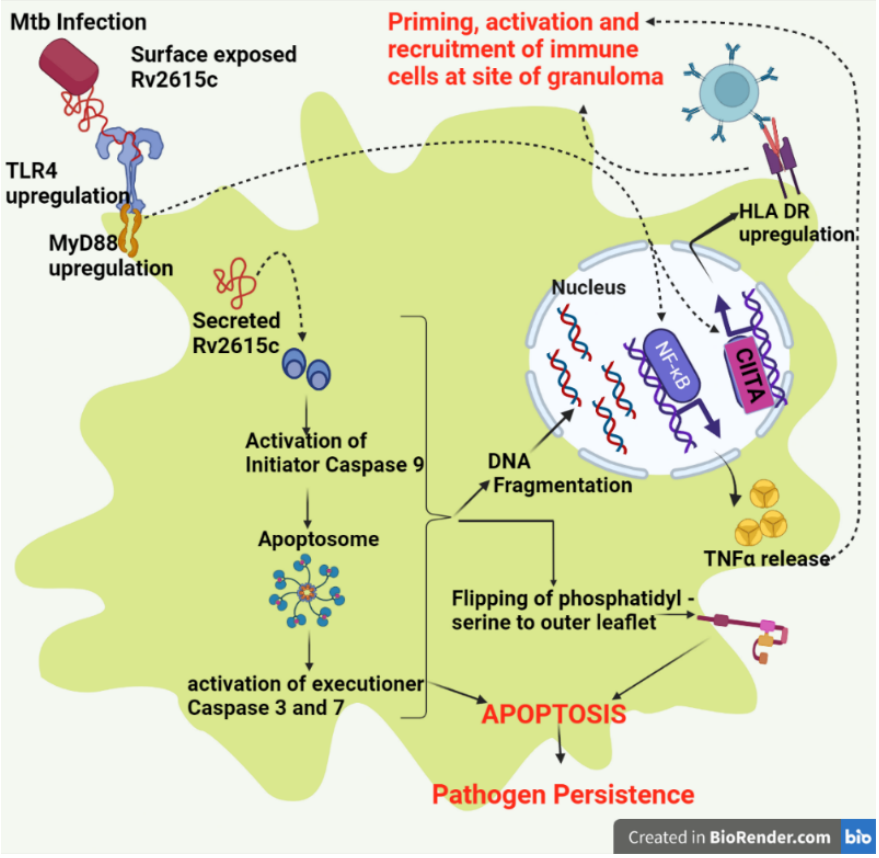

Figure 8. Schematic representation of immuno-modulatory role played by Rv2615c

Rv2615c can interact and activate the host immune receptor TLR4 leading to activation of downstream effectors such as MyD88, NF-B and TNF-α along with up-regulation of antigen presenting molecules HLA-DR. By possessing a eukaryotic CARD-like domain, Rv2615c could activate the initiator Caspase9 activity and formation of apoptosome complex which further activates executioner Caspase 3 and 7 and induces apoptosis. These observations implicate that Rv2615c could be a late stage expressing protein of Mtb facilitating cell-to spread of infection, activation and recruitment of immune cells at granuloma site and ultimately pathogen persistence.

4. Materials and Methods:

4.1 *In-silico* characterization of Rv2615c

4.1.1 Homology modelling and structure-based functional prediction of Rv2615c protein

The sequence of Rv2615c protein was retrieved from Mycobrowser and subjected to various servers for structure and function-based predictions. Antigenicity of Rv2615c was estimated in Vaxijen 2.0 server with a set threshold default value of 0.4 (Doytchinova and Flower, 2007).

The secondary structure and the structure-based function of Rv2615c protein was predicted using I-TASSER (Iterative Threading ASSEmbly Refinement) server. Structural analogs, Gene ontology (GO) template analogs and consensus GO terms for biological process and molecular functions were predicted (Roy, Kucukural and Zhang, 2010). Five homology-based models were predicted for Rv2615c. Chiron server was used for energy minimization of models (Ramachandran *et al.* , 2011). The output models were validated for their stereo-chemical quality through PROCHECK, VERIFY3D and ERRAT server (Lüthy, Bowie and Eisenberg,

1992; Laskowski *et al.* , 1996). PROCHECK confirms the quality of protein structure by Ramachandran plot where <5 residues in the disallowed region are considered to constitute a good structure. The best model of protein structure was selected with fewer residues in disallowed region of Ramachandran plot, high score in VERIFY3D and ERRAT.

4.2 In vitro assessment of Rv2615c potential for inducing apoptosis

4.2.1 Cloning, expression and purification of recombinant Rv2615c protein

Cloning, expression and purification of Rv2615c protein was performed as described in Medha *et al* ., (Medha, Joshi, *et al.* , 2022) (Medha, Priyanka, *et al.* , 2022).

Briefly, the Rv2615c gene was directly cloned in the pGEM-T Easy vector and its successful sequencing was verified. The full-length gene was then sub-cloned using BamHI and HindIII restriction enzymes in the expression vector pET-28a (+) in frame with a 6x histidine tag at the N-terminus. The target gene containing recombinant plasmid was introduced into *Escherichia coli (E. coli)* BL21 *DE3* for protein over-expression after being induced with 1mM IPTG and maintained at 37° 250 rpm for a couple of hours, then at 20° overnight. Culture was pelleted and re-suspended in 20-30 ml of 1XPBS+1mM PMSF followed by sonication (duty cycle 30; 5-6 cycles). Pellet was washed step wise with 10 ml 2%, 1% TritonX in PBS followed by 10ml 1X PBS and finally dissolved in Buffer (50mM NaH2PO4, 300 mMNacl, 8M Urea) and kept for binding at 4° with Ni-NTA matrix in column. Column was washed thrice with 1X cold PBS and wash fractions collected. Elution was performed with different gradients of immidazole. Elution buffer constituents: 50mM NaH2PO4, 300mM Nacl, 10mM TrisCl, 1mM PMSF, 10% glycerol, βMe, 8mM urea. SDS-PAGE was used to analyse the recombinant protein's purity, which was then validated by Coomassie Blue staining and immuno-blotting using anti-His antibodies. To remove immidazole and urea, purified protein was dialyzed against 1XPBS and decreasing urea concentrations. Purified recombinant proteins were then incubated for 1 h at 4°C with polymyxinB-agarose beads to remove endotoxin contamination. Limulus Amoebocyte Lysate (LAL) assay was performed using Peirce LAL assay kit following manufacturer's instructions to ensure negligible endotoxin levels in the purified protein (Pierce LAL Chromogenic Endotoxin Quantitation Kit, Cat no. 88282). The BCA protein assay was used to determine the protein content. Up to usage, the purified protein was kept in tiny aliquots at 80 °C.

4.2.2 Human Cell Culture: THP-1 cells stimulation with recombinant Rv2615c protein

In tissue culture plates, the human monocytic cell line THP-1 (NCCS, Pune) was cultured ($1X10^5$cells/ml cells per ml) in RPMI 1640, 10% foetal calf serum and an antibiotic cocktail that included penicillin (10,000 units/ml) and streptomycin (10,000 g/ml). For the purpose of differentiating the monocytic cells into macrophages, 40ng/ml Phorbol-Myristate Acetate (PMA; Sigma) was added to the monocytic cells and left overnight.

4.2.2 (a) Detection of Cell Viability Using MTT and Cell Titer blue

For dose dependent viability assessment, cells were stimulated with different concentration (5µg, 10µg, 15µg) of purified Rv2615c protein for 24h. For checking the viability in time dependent manner, unstimulated cells and cells stimulated with (10µg/ml) Rv2615c/(40ng/ml) LPS/(2µM) Staurosporine were incubated for 16h, 24h and 48h. Staurosporine is an alkaloid derivative from the bacterium *Streptomyces staurosporeus* which has been extensively been used as an inducer of apoptosis because it inhibits many different kinases.

Cells were exposed to either CellTiter Blue Reagent (20 mL/well) or MTT (5 mg/ml) and incubated for 4 hours at 37 °C and 5% CO2. Tetrazolium rings can be transformed into purple, insoluble formazan crystals by active dehydrogenases found in live cells. The crystals were dissolved in 100 µL of DMSO and the overall activity of bio-reductase enzyme was measured spectrophotometrically at (570-690) nm. The CellTiter-Blue Reagent constitutes of resazurin in a buffer solution. Resorufin (dark pink), which is extremely fluorescent and whose absorbance may be measured spectrophotometrically at (570–600) nm, can be reduced from resazurin (dark blue) by viable cells. The percentage of cell viability was calculated using the acquired absorbance values. Cells cultured in medium alone were thought to be completely viable.

4.2.2 (b) Lactate Dehydrogenase (LDH) release assay to identify cell cytotoxicity

Lactate dehydrogenase is a cytosolic enzyme which is released into the cell culture media with plasma membrane damage which can be measured. Levels of LDH released in the media are an indicator whether the cells are undergoing necrosis. High levels of LDH in the media are proportional to cell death via necrosis. Plates with unstimulated cells and Rv2615c or control (LPS/Staurosporine) stimulated cells were centrifuged and 20µl of media from each well and 20µl reaction buffer were added to fresh wells. Plates were incubated for 30 min at room temperature following addition of 20µl stop solution. Absorbance reading was recorded at 490nm.

4.2.2 (c) Detection of Phosphatidyl-serine Exposure by Annexin V-FITC Staining

Phosphatidylserine exposure, an early step of apoptosis induction in protein-stimulated THP-1 macrophages was estimated by Annexin V-FITC apoptosis detection kit (Thermo Scientific). Unstimulated and cells stimulated with Rv2615c and controls- (LPS/Staurosporine) were stained with AnnexinV-FITC and Propidium Iodide (PI) following manufacturer's protocol and analysed using flow cytometer (BD AccuriC6). Following stimulation time points of 16h, 24h and 48h; macrophages were collected after cold PBS washing and detached by scraping. After washing twice, the cells were re-suspended in binding buffer. An aliquot of 200 µl was mixed with 5 µl of Annexin V-FITC and 5 µl of PI. The mixture was incubated for 10 min at room temperature in the dark. Finally, the cells were analysed by flow cytometry.

4.2.2 (d) DNA Fragmentation analysis by TUNEL Assay

Unstimulated and cells stimulated with Rv2615c or controls- (LPS/Staurosporine) were incubated for different time points. Harvested cells were fixed in 1% paraformaldehyde and incubated for 60 minutes on ice. Fixed cells were washed first with ice-cold PBS followed by 70% ethanol and initially incubated for 30 minutes on ice and later on stored at -20 °C for 18h. Finally, for labelling DNA breaks to detect apoptosis; according to the manufacturer's instructions, cells were stained with the APO-Direct kit (BD Pharmingen) and analysed using the BD accuri C6 flow cytometer. Briefly, Cells were stained in reaction buffer constituting of Terminal de-oxynucleotidyltransferase (TdT) enzyme and fluoresceinated-dUTP (FITC-dUTP).

4.2.2 (e) Detection of activated initiator Caspase9

Total protein was extracted after 24 hours of protein stimulation by lysing THP-1 macrophages using RIPA lysis buffer and a protease inhibitor cocktail (Santa Cruz Biotechnology Ltd.). Equal concentrations of samples were analysed through SDS-PAGE before being transferred onto nitrocellulose membrane. The total protein content of the entire cell lysate was measured. Primary polyclonal antibody to Caspase9 (PAA627Hu03, Cloud-Clone Corp.), as well as GAPDH (Thermo Scientific) as an internal control, were incubated overnight in membranes after blocking for 1h in 5% skimmed milk dissolved in Tris-buffered saline with Tween 20 (TBST) buffer. Membranes were washed in TBST solution before being incubated for 1 hour with a secondary antibody that has been HRP-conjugated. To create the blot, an ECL Chemiluminescence Kit was employed (Thermo Scientific). Using ImageJ software, Western Blotting pictures were also quantified. Each sample's developed band area was examined, and graphs were drawn as a ratio to the Unstimulated sample.

4.2.2 (f) Detection of activated Caspases 3 and 7

For detection of activation of Caspase 3 and 7 which is a distinctive feature of early stages of apoptosis, CellEvent Caspase-3/7 Green Flow Cytometry Assay kit (Invitrogen) was used. Following incubation, unstimulated cells and cells stimulated with either Rv2615c or controls- (LPS/Staurosporine) were harvested and 500nM cell event Caspase 3/7 reagent was added to 1ml cell suspension in 1xPBS. Cells were incubated for 30 mins at 37°C. During final 5 mins of staining, 1µM SYTOX dead cell stain was added and samples were analysed in BD accuri C6 flow cytometer.

To confirm the observed apoptosis in response to Rv2615c to be Caspase dependent, Caspase inhibition studies were done. For inhibition study, cells were incubated with 20µM total Caspase inhibitor (Z-VAD-fmk; Promega) for 1 h, followed by treatment with respective test protein/controls and incubated for 24 h.

Percentage of Caspase 3 and 7 activation and percentage of AnnexinV and AnnexinV/PI dual positive cell population were analysed using flow cytometry.

4.3. Role of Rv2615c in immune response modulation via expression of TLR, HLA-DR and downstream effector molecules

4.3 (a) Predicting the identity of the TLR involved in Rv2615c interaction

The human TLR4 (PDB ID 3FXI) and TLR2 (PDB ID: 2Z7X) protein structures were obtained from the RCSB protein data bank. Rv2615c interactions with TLR4 and TLR2 were compared using HADDOCK 2.2 web server (van Zundert*et al.* , 2016). The active sites within the TLR and Rv2615c molecules were predicted using CastP server (Tian *et al.* , 2018). Site directed docking was performed and docked complex were evaluated on the basis of Z scores.

4.3 (b) Expression profile of TLRs and HLA-DR in response to Rv2615c

The expression profile of TLR2 and TLR4 was evaluated through flow cytometry following 24h stimulation of THP-1 macrophages with the 10µg/ml Rv2615c protein. The controls included were TLR4 agonist- LPS (40ng/ml) and TLR2 agonist- Cell Wall Fraction of H37Rv (CWF) (5µg/ml) (BEI Resources) (Manček-Keber and Jerala, 2015). Following incubation, cells were harvested and washed in PBS and stained with APC labelled anti-human TLR2 (CD282) antibody (Thermo Scientific) or APC labelled anti-human TLR4 (CD284) antibody (Thermo Scientific) and PE labelled anti-human HLA-DR antibody (Thermo Scientific). Cells were analysed in BD Accuri C6 flow Cytometer. Results were analysed on the basis of percentage of positively stained cells.

For inhibitor assay, 1h prior to stimulation; cells were blocked with Anti-TLR4 monoclonal antibody (Thermo Scientific) and analysed for expression of TLR4 and HLA-DR after 24h using flow cytometry.

4.3 (c) Expression profile of downstream effectors- MyD88 and NF-B using RT-PCR

mRNA was isolated from unstimulated and either Rv2615c (10µg/ml) or LPS (40ng/ml) stimulated THP-1 macrophages after 16h, 24h and 48h using mRNA synthesis kit (Promega Corporation) as per manufactures' protocol. 1µg of mRNA was converted to cDNA (Promega Corporation) using cDNA synthesis kit. mRNA and cDNA were checked by setting up PCR of endogenous control i.e., housekeeping gene GAPDH. Quantitative real time PCR for downstream effector genes- MyD88 and NF-B was performed by relative quantification in which the target concentration is expressed as ratio of target vs. reference gene (housekeeping gene GAPDH). The expression of MyD88 was evaluated following 24h of protein stimulation and the expression of NF-B was evaluated following 24h and 48h of protein stimulation. The primers used were Forward Primer 5' ATG GCT TCT ATG AGG CTG AG 3' and Reverse Primer 5' GTT GTTGTT GGT CTG GAT GC 3'. Equal concentration of cDNA for each sample was added to SYBR PCR master mix along with respective gene primers. 40 cycles of amplification followed by data acquisition and analysis was done. Data was calculated using the $2^{-[?][?]}$ CT method and are presented as fold induction. Fold change was normalized to GAPDH expression levels. Experiments were repeated thrice.

4.3 (d) Study of pro-inflammatory cytokine profile in response to Rv2615c

THP-1 macrophages were left unstimulated or stimulated with 10ug/ml of Rv2615c or control- LPS [40ng/ml] for 16h, 24h and 48h were analysed for secretion of TNFα (Thermo Scientific) and IL-1β (Biolegend) in cell culture supernatants. ELISA was done according to manufacturer's instructions.

ELISA was also performed for estimation of TNFα and IL-1β in supernatants blocked with Anti-TLR4 monoclonal antibody prior to stimulation with Rv2615c/controls till 24 h.

Statistical analysis

All the experiments were performed in triplicates. The results of all the experimental data are presented as Mean±SEM. GraphPad Prism version 5.02 was used to do statistical comparisons employing Student's

t-test (San Diego, CA, USA). Mean differences were analysed and * was used to represent the comparison with unstimulated control. Differences were considered significant at *P<0.05, **P<0.01, ***P<0.001.

4.4 Sequence scanning of Rv2615c protein

Predictions of I-TASSER strongly suggested the similarity of Rv2615c with APAF1-apoptosome structure involved in Caspase activation and cell death pathways followed by *in-vitro* experiments which further confirmed the apoptogenic role played by Rv2615c protein. It is reported that the APAF1-apoptosome activates the Caspase9 via CARD-CARD interaction between APAF1-Caspase9. Therefore, multiple sequence alignment of Rv2615c was performed with CARD-APAF1 and CARD-Caspase9. The alignment was checked for various conserved and similar residues. Secondary structure of predicted CARD-like domain in Rv2615c was analysed with MINNOU server (Cao *et al.* , 2006). Structural superimposition of predicted CARD-like domain in Rv2615c with CARD-APAF1 and CARD-Caspase9 was carried out in Pymol software.

4.4.1 Evaluating the binding affinity of CARD-like domain of Rv2615c with CARD-APAF1 and CARD-Caspase9

Molecular docking of Rv2615c protein was performed to estimate the binding affinity of CARD-like domain of Rv2615c with CARD-APAF1 and CARD-Caspase9 using PatchDock server (Schneidman-Duhovny *et al.* , 2005). Top ten docked structures were further refined in FireDock server (Mashiach *et al.* , 2008). The best model was evaluated based on number of bonds formed and the energy score generated in HEX 8.0.0. Visualization was done in Discovery studio Visualizer 4.1 (Accelyrs Inc., USA). The complex of CARD-APAF1 with CARD-Caspase9 (PDB ID: 3YGS) was included as positive control and the inactivated independent APAF-ADP complex (PDB ID: 1Z6T) was included as negative control in the study.

We observed Leucine-116 and Isoleucine-117 were two common residues within CARD-like domain of Rv2615c which aligned with conserved residues Methionine-29 and Isoleucine-30 of CARD-APAF1 and Leucine-58 and Isoleucine-59 of CARD-Caspase9. Therefore, site directed mutation was incorporated changing Leucine-116 and Isoleucine-117 to the most preferred Alanine substitution in CARD-like domain of Rv2615c and the mutant structure was checked for its stability using I-Mutant 2.0 server (Capriotti, Fariselli and Casadio, 2005). Furthermore, binding affinity of this mutant Rv2615c protein with CARD-APAF1 and with CARD-Caspase9 was evaluated through docking studies as described previously.

4.4.2 MD simulation of docked complexes

MD simulation for 100 nanoseconds (ns) using Gromacs software 2020.5 was performed to evaluate the stability of docked complexes of whole Rv2615c protein with CARD-APAF1 and CARD-Caspase9 separately and mutant Rv2615c with CARD-APAF1 and CARD-Caspase9 separately. The docked structure of APAF1-CARD and Caspase9-CARD (PDB ID: 3YGS) was included as positive control in the simulation studies. The docked complex was solvated by TIP3P [transferable intermolecular potential with 3 points] water model using CHARMM36 force field. The final MD simulation run was performed at 300K temperature and standard pressure of 1.01 bar using NPT (number of particle [N], system pressure [P] and temperature [T]) and NVT (number of particle [N], system volume [V] and temperature [T]) ensemble. Backbone Root Mean Square Deviation (RMSD) and Root Mean Square Fluctuation (RMSF) of the entire complex was calculated and plotted.

Acknowledgement

We acknowledge Department of Science and Technology (DST), Government of India, for providing financial assistance under Grant Sanction No. EMR/2016/006774. The Council of Scientific and Industrial Research [CSIR], Government of India, awarded Senior Research Fellowships to Medha and Priyanka. Professor Vikas Jain of the Indian Institute of Science Education and Research [IISER], Bhopal, is sincerely acknowledged for his direction and assistance in carrying out MD simulation research.

Author's Contributions

Monika Sharma led in conceptualization and funding acquisition. Medha contributed in conceptualization, execution of all the *in-silico*studies, and writing of the manuscript. Medha and Priyanka conducted all the experiments. Monika Sharma, Medha and Sadhna Sharma contributed in reviewing and editing of the manuscript.

Conflict of interest

The authors have no competing interests to declare.

Data Availability Statement

The datasets generated during and/or analysed during the current study are included in this article (and its supplementary information files). A descriptive dataset can be provided by the corresponding author upon reasonable request.

Compliance with Ethical Standards

This article does not contain any studies with human participants or animals performed by any of the authors.

References

Abdallah, A.M. *et al.* (2007) 'Type VII secretion–mycobacteria show the way.', *Nature reviews. Microbiology* , 5(11), pp. 883–891. Available at: https://doi.org/10.1038/nrmicro1773.

Abdallah, A.M. *et al.* (2011) 'Mycobacterial Secretion Systems ESX-1 and ESX-5 Play Distinct Roles in Host Cell Death and Inflammasome Activation', *The Journal of Immunology* , 187(9), pp. 4744 LP – 4753. Available at: https://doi.org/10.4049/jimmunol.1101457.

Aguilo, J.I. *et al.* (2013) 'ESX-1-induced apoptosis is involved in cell-to-cell spread of Mycobacterium tuberculosis', *Cellular Microbiology* , 15(12), pp. 1994–2005. Available at: https://doi.org/10.1111/cmi.12169.

Amaral, E.P. and Andrade, B.B. (2017) 'Nuclear Factor ϰ B Activation Pathways During Mycobacterium tuberculosis Infection'. Available at: https://doi.org/10.1177/1179568917695833.

Augenstreich, J. *et al.* (2017) 'ESX-1 and phthiocerol dimycocerosates of Mycobacterium tuberculosis act in concert to cause phagosomal rupture and host cell apoptosis', *Cellular Microbiology* , 19(7), p. e12726. Available at: https://doi.org/10.1111/cmi.12726.

Bansal, K. *et al.* (2010) 'PE_PGRS Antigens of Mycobacterium tuberculosis Induce Maturation and Activation of Human Dendritic Cells',*The Journal of Immunology* , 184(7), pp. 3495 LP – 3504. Available at: https://doi.org/10.4049/jimmunol.0903299.

Basu, S. *et al.* (2007) 'Execution of macrophage apoptosis by PE_PGRS33 of Mycobacterium tuberculosis is mediated by toll-like receptor 2-dependent release of tumor necrosis factor-α', *Journal of Biological Chemistry* , 282(2), pp. 1039–1050. Available at: https://doi.org/10.1074/jbc.M604379200.

Brennan, M.J. (2017) 'The Enigmatic PE/PPE Multigene Family of Mycobacteria and Tuberculosis Vaccination', *Infection and Immunity* . Edited by A.T. Maurelli, 85(6), pp. e00969-16. Available at: https://doi.org/10.1128/IAI.00969-16.

Cadieux, N. *et al.* (2011) 'Induction of cell death after localization to the host cell mitochondria by the Mycobacterium tuberculosis PE_PGRS33 protein', *Microbiology* , 157(3), pp. 793–804. Available at: https://doi.org/10.1099/mic.0.041996-0.

Cao, B. *et al.* (2006) 'Enhanced recognition of protein transmembrane domains with prediction-based structural profiles.',*Bioinformatics (Oxford, England)* , 22(3), pp. 303–309. Available at: https://doi.org/10.1093/bioinformatics/bti784.

Capriotti, E., Fariselli, P. and Casadio, R. (2005) 'I-Mutant2.0: predicting stability changes upon mutation from the protein sequence or structure.', *Nucleic acids research* , 33(Web Server issue), pp. W306-10. Available at: https://doi.org/10.1093/nar/gki375.

Chai, Q. *et al.* (2019) 'A Mycobacterium tuberculosis surface protein recruits ubiquitin to trigger host xenophagy.', *Nature communications* , 10(1), p. 1973. Available at: https://doi.org/10.1038/s41467-019-09955-8.

Chai, Q., Wang, L. and Liu, C.H. (2020) 'New insights into the evasion of host innate immunity by Mycobacterium tuberculosis', *Cellular & Molecular Immunology* [Preprint], (July). Available at: https://doi.org/10.1038/s41423-020-0502-z.

Chen, T. *et al.* (2013) 'Mycobacterium tuberculosis PE_PGRS17 promotes the death of host cell and cytokines secretion via Erk kinase accompanying with enhanced survival of recombinant Mycobacterium smegmatis.', *Journal of interferon & cytokine research : the official journal of the International Society for Interferon and Cytokine Research* , 33(8), pp. 452–458. Available at: https://doi.org/10.1089/jir.2012.0083.

Chmiela, M. and Gonciarz, W. (2017) 'Molecular mimicry in Helicobacter pylori infections', *World journal of gastroenterology* , 23(22), pp. 3964–3977. Available at: https://doi.org/10.3748/wjg.v23.i22.3964.

Cole, S.T. *et al.* (1998) 'Deciphering the biology of Mycobacterium tuberculosis from the complete genome sequence',*Nature* , 393(6685), pp. 537–544. Available at: https://doi.org/10.1038/31159.

Davis, J.M. *et al.* (2002) 'Real-time visualization of mycobacterium-macrophage interactions leading to initiation of granuloma formation in zebrafish embryos', *Immunity* , 17(6), pp. 693–702.

Desler, C. *et al.* (2009) 'In Silico screening for functional candidates amongst hypothetical proteins', *BMC Bioinformatics* , 10(1), p. 289. Available at: https://doi.org/10.1186/1471-2105-10-289.

Dorhoi, A. and Kaufmann, S.H.E. (2014) 'Tumor necrosis factor alpha in mycobacterial infection', *Seminars in Immunology* , 26(3), pp. 203–209. Available at: https://doi.org/https://doi.org/10.1016/j.smim.2014.04.003.

Doytchinova, I.A. and Flower, D.R. (2007) 'VaxiJen: a server for prediction of protective antigens, tumour antigens and subunit vaccines.', *BMC bioinformatics* , 8, p. 4. Available at: https://doi.org/10.1186/1471-2105-8-4.

Fayyazi, A. *et al.* (2000) 'Apoptosis of macrophages and T cells in tuberculosis associated caseous necrosis', *The Journal of pathology* , 191(4), pp. 417–425.

Gey Van Pittius, N.C. *et al.* (2006) *Evolution and expansion of the Mycobacterium tuberculosis PE and PPE multigene families and their association with the duplication of the ESAT-6 (esx) gene cluster regions* , *BMC Evolutionary Biology* . Available at: https://doi.org/10.1186/1471-2148-6-95.

Gleeson, L.E. *et al.* (2016) 'Cutting Edge: Mycobacterium tuberculosis Induces Aerobic Glycolysis in Human Alveolar Macrophages That Is Required for Control of Intracellular Bacillary Replication',*The Journal of Immunology* , 196(6), pp. 2444 LP – 2449. Available at: https://doi.org/10.4049/jimmunol.1501612.

Grover, S. *et al.* (2018) 'The PGRS domain of Mycobacterium tuberculosis PE_PGRS protein Rv0297 is involved in Endoplasmic reticulum stress-mediated apoptosis through toll-like receptor 4',*mBio* , 9(3). Available at: https://doi.org/10.1128/mBio.01017-18.

Hackett, E.E. *et al.* (2020) 'Mycobacterium tuberculosis Limits Host Glycolysis and IL-1β by Restriction of PFK-M via MicroRNA-21',*Cell Reports* , 30(1), pp. 124-136.e4. Available at: https://doi.org/https://doi.org/10.1016/j.celrep.2019.12.015.

Hasan, S. *et al.* (2006) 'Prioritizing Genomic Drug Targets in Pathogens: Application to Mycobacterium tuberculosis', *PLOS Computational Biology* , 2(6), p. e61. Available at: https://doi.org/10.1371/journal.pcbi.0020061.

Horng, T. *et al.* (2002) 'The adaptor molecule TIRAP provides signalling specificity for Toll-like receptors', *Nature* , 420(6913), pp. 329–333. Available at: https://doi.org/10.1038/nature01180.

Hu, Q. *et al.* (2014) 'Molecular determinants of caspase-9 activation by the Apaf-1 apoptosome', *Proceedings of the National Academy of Sciences of the United States of America* . 2014/10/13, 111(46), pp. 16254–16261. Available at: https://doi.org/10.1073/pnas.1418000111.

Kruh, N.A. *et al.* (2010) 'Portrait of a Pathogen: The Mycobacterium tuberculosis Proteome In Vivo', *PLOS ONE* , 5(11), p. e13938. Available at: https://doi.org/10.1371/journal.pone.0013938.

Kumar, K. *et al.* (2014) 'Functional annotation of putative hypothetical proteins from Candida dubliniensis', *Gene* , 543(1), pp. 93–100. Available at: https://doi.org/https://doi.org/10.1016/j.gene.2014.03.060.

Laskowski, R.A. *et al.* (1996) 'AQUA and PROCHECK-NMR: programs for checking the quality of protein structures solved by NMR.',*Journal of biomolecular NMR* , 8(4), pp. 477–486. Available at: https://doi.org/10.1007/BF00228148.

Li, H. *et al.* (2016) 'Mycobacterium tuberculosis PE13 (Rv1195) manipulates the host cell fate via p38-ERK-NF-κB axis and apoptosis',*Apoptosis : an international journal on programmed cell death* , 21(7), pp. 795–808. Available at: https://doi.org/10.1007/s10495-016-1249-y.

Liu, S. *et al.* (2020) 'PE_PGRS31-S100A9 Interaction Promotes Mycobacterial Survival in Macrophages Through the Regulation of NF-κB-TNF-α Signaling and Arachidonic Acid Metabolism.', *Frontiers in microbiology* , 11, p. 845. Available at: https://doi.org/10.3389/fmicb.2020.00845.

Lüthy, R., Bowie, J.U. and Eisenberg, D. (1992) 'Assessment of protein models with three-dimensional profiles.', *Nature* , 356(6364), pp. 83–85. Available at: https://doi.org/10.1038/356083a0.

Manček-Keber, M. and Jerala, R. (2015) 'Postulates for validating TLR4 agonists', *European Journal of Immunology* , 45(2), pp. 356–370. Available at: https://doi.org/https://doi.org/10.1002/eji.201444462.

Mashiach, E. *et al.* (2008) 'FireDock: a web server for fast interaction refinement in molecular docking', *Nucleic acids research* . 2008/04/19, 36(Web Server issue), pp. W229–W232. Available at: https://doi.org/10.1093/nar/gkn186.

McGuire, A.M. *et al.* (2012) 'Comparative analysis of mycobacterium and related actinomycetes yields insight into the evolution of mycobacterium tuberculosis pathogenesis', *BMC Genomics* , 13(1). Available at: https://doi.org/10.1186/1471-2164-13-120.

Medha, Joshi, H., *et al.* (2022) 'Elucidating the function of hypothetical PE_PGRS45 protein of Mycobacterium tuberculosis as an oxido-reductase: a potential target for drug repurposing for the treatment of tuberculosis', *Journal of Biomolecular Structure and Dynamics* , pp. 1–17.

Medha, Priyanka, *et al.* (2022) 'Role of C-terminal domain of Mycobacterium tuberculosis PE6 (Rv0335c) protein in host mitochondrial stress and macrophage apoptosis.', *Apoptosis : an international journal on programmed cell death* , pp. 1–30. Available at: https://doi.org/10.1007/s10495-022-01778-1.

Medha, Sharma, S. and Sharma, M. (2021) 'Acta Tropica Proline-Glutamate / Proline-Proline-Glutamate (PE / PPE) proteins of Mycobacterium tuberculosis : The multifaceted immune-modulators', *Acta Tropica* , 222(April), p. 106035. Available at: https://doi.org/10.1016/j.actatropica.2021.106035.

Mishra, B.B. *et al.* (2010) 'Mycobacterium tuberculosis protein ESAT-6 is a potent activator of the NLRP3/ASC inflammasome',*Cellular Microbiology* , 12(8), pp. 1046–1063. Available at: https://doi.org/https://doi.org/10.1111/j.1462-5822.2010.01450.x.

Murphy, D.J. and Brown, J.R. (2007) 'Identification of gene targets against dormant phase Mycobacterium tuberculosis infections', *BMC Infectious Diseases* , 7(1), p. 84. Available at: https://doi.org/10.1186/1471-2334-7-84.

Pan, H. *et al.* (2005) 'Ipr1 gene mediates innate immunity to tuberculosis', *Nature* , 434(7034), pp. 767–772.

Próchnicki, T. and Latz, E. (2017) 'Inflammasomes on the Crossroads of Innate Immune Recognition and Metabolic Control', *Cell Metabolism* , 26(1), pp. 71–93. Available at: https://doi.org/https://doi.org/10.1016/j.cmet.2017.06.018.

Ramachandran, S. *et al.* (2011) 'Automated minimization of steric clashes in protein structures.', *Proteins* , 79(1), pp. 261–270. Available at: https://doi.org/10.1002/prot.22879.

Ramakrishnan, L. (2012) 'Revisiting the role of the granuloma in tuberculosis', *Nature Reviews Immunology* , 12(5), pp. 352–366.

Roy, A., Kucukural, A. and Zhang, Y. (2010) 'I-TASSER: a unified platform for automated protein structure and function prediction',*Nature Protocols* , 5(4), pp. 725–738. Available at: https://doi.org/10.1038/nprot.2010.5.

Saini, N.K. *et al.* (2016) 'Suppression of autophagy and antigen presentation by Mycobacterium tuberculosis PE_PGRS47', *Nature Microbiology* , 1(9), p. 16133. Available at: https://doi.org/10.1038/nmicrobiol.2016.133.

Sánchez, D. *et al.* (2010) 'Role of TLR2- and TLR4-mediated signaling in Mycobacterium tuberculosis-induced macrophage death',*Cellular Immunology* , 260(2), pp. 128–136. Available at: https://doi.org/https://doi.org/10.1016/j.cellimm.2009.10.007.

Saraav, I. *et al.* (2017) 'Mycobacterium tuberculosis MymA is a TLR2 agonist that activate macrophages and a TH1 response',*Tuberculosis* , 106, pp. 16–24. Available at: https://doi.org/https://doi.org/10.1016/j.tube.2017.05.005.

Saunders, B.M. and Britton, W.J. (2007) 'Life and death in the granuloma: immunopathology of tuberculosis', *Immunology & Cell Biology* , 85(2), pp. 103–111. Available at: https://doi.org/10.1038/sj.icb.7100027.

Schneidman-Duhovny, D. *et al.* (2005) 'PatchDock and SymmDock: servers for rigid and symmetric docking', *Nucleic acids research* , 33(Web Server issue), pp. W363–W367. Available at: https://doi.org/10.1093/nar/gki481.

Seimon, T.A. *et al.* (2010) 'Induction of ER Stress in Macrophages of Tuberculosis Granulomas', *PLOS ONE* , 5(9), p. e12772. Available at: https://doi.org/10.1371/journal.pone.0012772.

Sharma, N. *et al.* (2021) 'Mycobacterium tuberculosis Protein PE6 (Rv0335c), a Novel TLR4 Agonist, Evokes an Inflammatory Response and Modulates the Cell Death Pathways in Macrophages to Enhance Intracellular Survival', *Frontiers in immunology* , 12, p. 696491. Available at: https://doi.org/10.3389/fimmu.2021.696491.

Sonia, M. *et al.* (2021) 'Molecular Mimicry: a Paradigm of Host-Microbe Coevolution Illustrated by Legionella', *mBio* , 11(5), pp. e01201-20. Available at: https://doi.org/10.1128/mBio.01201-20.

Tian, W. *et al.* (2018) 'CASTp 3.0: computed atlas of surface topography of proteins.', *Nucleic acids research* , 46(W1), pp. W363–W367. Available at: https://doi.org/10.1093/nar/gky473.

Tiwari, B., Ramakrishnan, U.M. and Raghunand, T.R. (2015) 'The Mycobacterium tuberculosis protein pair PE9 (Rv1088)–PE10 (Rv1089) forms heterodimers and induces macrophage apoptosis through Toll-like receptor 4', *Cellular Microbiology* , 17(11), pp. 1653–1669. Available at: https://doi.org/10.1111/cmi.12462.

Urán Landaburu, L. *et al.* (2020) 'TDR Targets 6: driving drug discovery for human pathogens through intensive chemogenomic data integration', *Nucleic Acids Research* , 48(D1), pp. D992–D1005. Available at: https://doi.org/10.1093/nar/gkz999.

Volkman, H.E. *et al.* (2004) 'Tuberculous Granuloma Formation Is Enhanced by a Mycobacterium Virulence Determinant', *PLOS Biology* , 2(11), p. e367. Available at: https://doi.org/10.1371/journal.pbio.0020367.

WHO (2021) *WHO Global TB Report* . World Health Organization.

Yamamoto, M. *et al.* (2002) 'Essential role for TIRAP in activation of the signalling cascade shared by TLR2 and TLR4',*Nature* , 420(6913), pp. 324–329. Available at: https://doi.org/10.1038/nature01182.

van Zundert, G.C.P. *et al.* (2016) 'The HADDOCK2.2 Web Server: User-Friendly Integrative Modeling of Biomolecular Complexes.',*Journal of molecular biology* , 428(4), pp. 720–725. Available at: https://doi.org/10.1016/j.jmb.2015.09.014.